Journal of Translational Medicine

RESEARCH

Open Access

The integrative genomic and functional immunological analyses of colorectal cancer initiating cells to modulate stemness properties and the susceptibility to immune responses

Issam Tout[1], Salim Bougarn[1], Mohammed Toufiq[2], Neha Gopinath[1], Ola Hussein[1,3], Abbirami Sathappan[4], Evonne Chin-Smith[1], Fazulur Rehaman[5], Rebecca Mathew[5], Lisa Mathew[5], Kun Wang[5], Li Liu[5], Abdulrahman Salhab[5], Oleksandr Soloviov[5], Sara Tomei[5], Waseem Hasan[6], Sahar Da'as[6,7], Yosra Bejaoui[7], Nady El Hajj[7], Karama Makni Maalej[8], Said Dermime[8], Kakil Rasul[9], Paolo Dellabona[10], Giulia Casorati[10], Alice Turdo[11], Matilde Todaro[11], Giorgio Stassi[12], Soldano Ferrone[13], Xinhui Wang[13] and Cristina Maccalli[1,7*]

Abstract

Background Colorectal cancer (CRC) initiating cells (CICs) possess self-renewal capabilities and are pivotal in tumor recurrence and resistance to conventional therapies, including immunotherapy. The mechanisms underlying their interaction with immune cells remain unclear.

Methods We conducted a multi-omics analysis—encompassing DNA methylation, total RNA sequencing, and microRNAs (miRNAs; N = 800) profiling on primary CICs and differentiated tumor cell lines, including autologous pairs. Functional immunological assays were performed to assess the impact of miRNA modulation.

Results CICs exhibited distinct methylation patterns, transcriptomic profiles, and miRNA expressions compared to differentiated tumor cells ($p < 0.05$ or 0.01). Notably, miRNA-15a and -196a were implicated in regulating tumorigenic pathways, such as epithelial-to-mesenchymal transition (EMT), TGF-β signaling, and immune modulation. The transfection of CICs with miRNA mimics led to the downregulation of oncogenic EMT markers (*CRKL*, *lncRNA SOX2-OT*, *JUNB*, *SMAD3*) and TGF-β pathway, resulting in a significant reduction of the in vitro proliferation and the tumorigenicity and migration in a zebrafish xenograft model. Additionally, miRNA-15a enhanced the expression of antigen processing machinery and decreased the expression of immune checkpoints (PD-L1, PD-L2, CTLA-4) and immunosuppressive cytokines (IL-4). The co-culture of HLA-matched lymphocytes with CICs overexpressing the miRNA-15a, elicited robust tumor-specific immune responses, characterized by a shift toward central and effector memory T cell phenotypes and prevented their terminal differentiation and exhaustion. The combination of miRNA modulation with Indoleamine 2,3-dioxygenase blockade and immunomodulating agents further potentiated these effects.

Conclusions Our study demonstrates that the modulation of miRNA-15a in CICs not only suppresses the tumorigenic properties but also enhances their visibility to the immune system by upregulating antigen presentation and reducing immunomodulatory molecules. These findings suggest that combining miRNA modulation with epigenetic or immunomodulatory agents holds significant promise for overcoming treatment resistance in CRC.

*Correspondence:
Cristina Maccalli
cmaccalli@sidra.org
Full list of author information is available at the end of the article

Keywords Colorectal cancer, Cancer initiating cells, MicroRNAs, T-cell responses, Combination therapies

Graphical Abstract

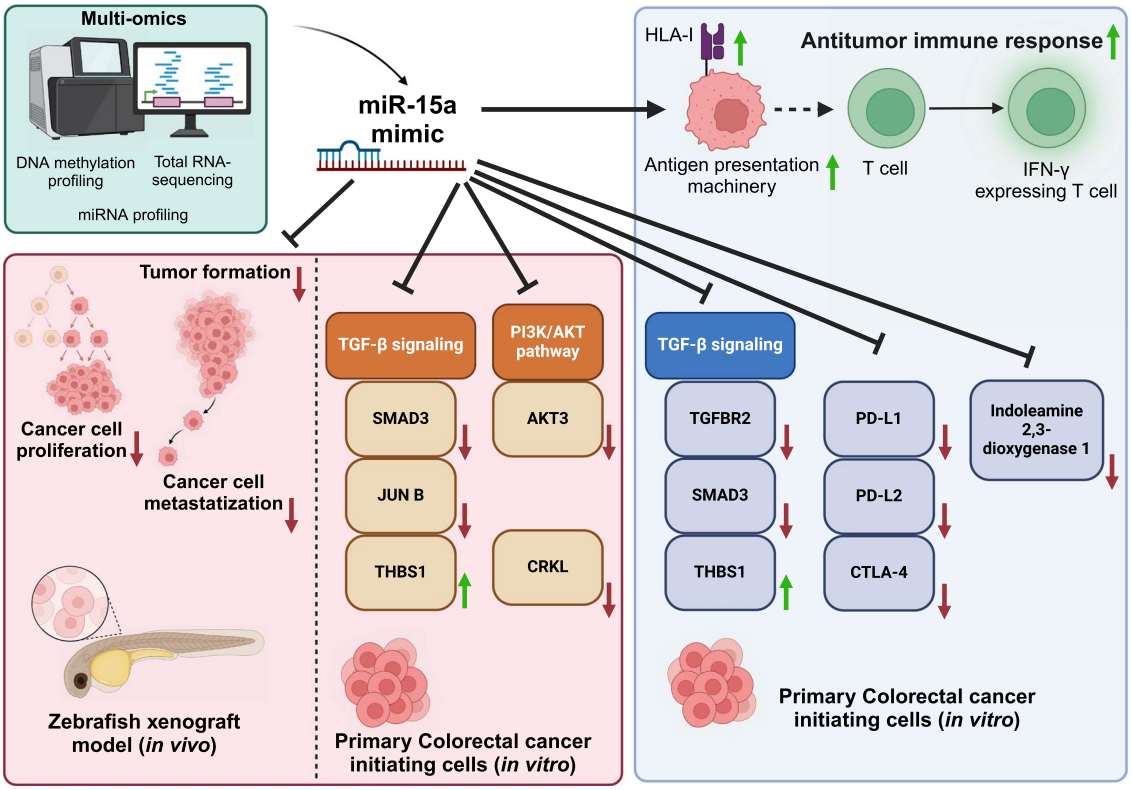

Introduction

Colorectal cancer (CRC) is the third most common cancer worldwide and is responsible for around 0.5 million deaths per year [1]. The combination of different standard therapeutic regimens and the advent of targeted therapies and immunotherapy has improved the overall survival (OS) for these patients; nevertheless, a significant proportion of patients shows either resistance to these therapeutic strategies or acquired resistance in the course of treatments [2].

Among different subpopulations that compose the tumors, a minority is endowed with "stemness" and tumor initiating properties [3]. These cells, denominated cancer initiating cells or cancer stem cells (CICs/CSCs) display characteristics of self-renewal, quiescence and pluripotency which drive the initiation and maintenance of the tumor. Moreover, this subpopulation of cancer cells is considered responsible for disease metastatization and resistance to therapies [4]. Multiple markers, e.g. CD133, CD24, EpCAM, ALDH-1, and few targets of Wnt signaling (e.g., Lgr5 and CD44v6) are expressed by CRC-CICs [4, 5]. However, most of these markers are shared with normal cells or reflect different stages of cell proliferation and/or differentiation highlighting the plasticity and the high grade of heterogeneity at intra- and inter-cancer levels [6, 7].

Cancer immunotherapy, including immune checkpoint inhibitors, adoptive cell therapies, and tumor vaccines, have demonstrated remarkable clinical efficacy for the treatment of various types of cancer [8, 9]. T cells, which recognize specific tumor antigen-derived peptides presented by the human leukocyte antigen (HLA) molecules on the membrane of tumor cells, play a pivotal mechanism of action for many of these therapies. However, tumor cells escape from immune responses, through the loss or suboptimal expression of HLA or antigen processing machinery (APM) molecules [10]. Loss of the expression of MHC class I has been correlated with resistance to either immune checkpoint blockade [11] or adoptive immunotherapy [12]. The poor immunological profile of

CICs isolated from solid tumors with different histological origins, including CRC, has been previously reported, with common detection of suboptimal expression of HLA and APM molecules [4, 13]. Additional mechanisms of immune evasion by CICs include the expression of IL-4 and immune checkpoint molecules, that in some cases were detected at superior levels in CICs as compared to bulk tumor cells [14].

Epigenetic drugs, such as inhibitors of DNA methyltransferases, the enzymes that are responsible for DNA methylation [15], and thereby reversing gene silencing through the demethylation of promoters, can increase the expression of MHC class I molecules, and potentiate the efficacy of anti-tumor immune responses [16]. 5-Azacytidine (5-aza) is a common DNA demethylating anticancer drug, mainly used for the treatment of various types of cancer, including breast cancer, leukemia and CRC [17]. Other epigenetic therapies include the histone deacetylase (HDAC) inhibitors (HDACis), that, through the removal of acetyl groups from histone lysine residues, modulate the chromatin structure and influence the transcription of genes. HDAC dysregulation occurs across various cancer subtypes, and HDACis represent promising anticancer therapies, with few of them (e.g., Vorinostat and Dorminostat) being approved by the Food and Drug Administration (FDA) for the treatment of hematological malignancies [18]. These agents have been shown to modulate the immunogenicity of tumor cells [19], although limited efficacy has been reported for solid tumors [20]. The suboptimal modulation by either IFN-γ or 5-aza of the levels of HLA molecules in CICs has been also reported [21].

Micro RNAs (miRNAs), that are small non-coding RNAs consisting of 18–25 nucleotides, can regulate the translation of genes associated with multiple pathways. MiRNAs recognize the complementary sequences in the 3′ untranslated regions (3′UTR) of given mRNAs to cause their degradation, translational repression or positive regulation [22]. Abnormal expression of miRNAs, resulted by genetic and/or epigenetic alterations, is frequently observed in various cancer types, impacting cancer pathogenesis [23] and also providing novel targets for the therapeutic modulation of tumor cell behavior. MiRNAs regulating stemness functions have been isolated in different types of solid tumors, including CRC [24]. Moreover, miRNAs are critically implicated in tuning both cancer cell immunogenicity and general immune responses [25]. However, the effect of either epigenetic agents or miRNAs in modulating the immunogenicity and the susceptibility of CICs to immune responses still needs to be defined.

In this study, a deep genomic characterization, including DNA methylation, total RNA sequencing and miRNA profiling, of primary CICs and differentiated tumor cell lines isolated from CRC patients, has been performed and the results have been integrated with the functional in vitro assessment of stemness phenotype and immunological properties. The role of miRNAs-15a and -196a, which were differentially expressed in primary CICs vs. differentiated bulk tumor cells, in modulating the stemness and immunological profile of these cells has been determined., The modulation of miRNAs, either alone or in combination with epigenetic or immunomodulatory agents, by targeting the TGF-β pathway and the increased expression of HLA and APM molecules in tumor cells, could induce efficient T cell-mediated recognition of CICs. In addition, the regulatory activity of these agents on stemness and tumorigenicity were corroborated in vivo model of zebrafish xenograft.

Materials and methods

Cell lines and culture conditions

CRC-CICs and differentiated bulk tumor cell line (hereafter denominated FBS tumor cells) pairs (#1076, 1247, 111011, 14583) or tumor cell lines (1869 col and 1872 col) were previously isolated by C. Maccalli from biopsies of patients with diagnosis of CRC and admitted for surgery at the San Raffaele Hospital, Milan, Italy or at the National Cancer Center, NIH, Bethesda, MD, US [26]. Additional primary CICs were kindly provided by Drs. Giorgio Stassi and Matilde Todaro, University of Palermo, Italy, (CIC-2, 3, 5, 7, 8, 9, 11, 13, 14, 16, 20, 21, 33, 57 and 59) [26]. The cell lines SW620 (Cat# CCL-227; RRID: CVCL_0547) and SW480 (Cat #CCL-228; RRID: CVCL_0546) were obtained from ATCC (Manassas, Virginia). CICs were cultured as colon-spheres in Advanced DMEM/F12 medium (ThermoFisher, Cat #12634028) containing 20 ng/ml of epidermal growth factor (EGF PeproTech, Rocky Hill, NJ, Cat AF-100-15), 50 ng/ml fibroblast growth factor-2 (FGF-2; PeproTech, Rocky Hill, NJ, Cat AF-100-18), and other supplements as previously described [14]. The differentiated tumor cells were cultured in vitro as described in Volonte' et al. [14]. Genomic sequencing and HLA phenotyping were performed to check the identity and origins of the cell lines. Moreover, the absence of mycoplasma contamination, through RT-PCR with specific primers [14], has been regularly assessed along the cell culture of the cell lines. Peripheral blood lymphocytes isolated from healthy donors (HD) were obtained from STEMCELL Technologies (Vancouver, BC, CA).

Flow cytometry

The phenotype characterization of stemness and immune related markers of CICs vs. FBS tumor cells or the activation and differentiation of T lymphocytes was

performed according to the methods described *in S1–S3 sections of Supplemental materials.* Samples were acquired either with Navios (Beckman Coulter; RRID: SCR_023797) or with Cytek Aurora (Cytek; RRID: SCR_019826) flow cytometers and were analyzed either with FCS Express (De Novo Software; RRID: SCR_016431) or Kaluza (Beckman Coulter; RRID: SCR_016182) software.

Treatment of tumor cell lines with immunomodulating or epigenetic agents

Cells were cultured at a concentration of 0.2×10^6 cells/ml in 6-well plates with 5 ml/well of specific CIC or FBS medium and incubated with the following agents: IFN-γ (1000 IU/ml; Peprotech, Cat # 300-02-500) for 48 h; Vorinostat (1.25 µM, Selleckchem, Cat #S104713), Mithramycin A (0.3 µM, Sigma, Cat # 1489/1), RG108 (5 µM, Selleckchem, Cat #S2821) and 5-azacytidine (5-Aza, 5 µM, Selleckchem, Cat #S1782) for 24 h; Butyrate (1 mM, Stemcell, Cat #72242) for 12 h. The agents were dissolved according to the manufacturers' guidelines.

Genomics profiling of the cell lines

DNA and RNA extraction and purification from CICs and FBS cell lines were performed using the AllPrep DNA/RNA Mini Kit (Qiagen, Cat #80204). The amount and the quality of nucleic acids have been assessed by the Nanodrop 8000 and Qubit PicoGreen assay (ThermoScientific, Waltham, MA, USA; RRID: SCR_018600), and RNA RIN threshold has been determined by the 2100 BioAnalyzer (Agilent Technologies, Santa Clara, CA, USA; RRID: SCR_018043). Samples have been then processed for genomic analyses in a maximum of two batches of experimental runs. DNA methylation analysis was performed with the Infinium Methylation EPIC V.1 BeadChip (Illumina, San Diego, CA, USA; RRID: SCR_010958), upon bisulfite conversion of DNA through the EZ kit (Zymo Research; RRID: SCR_001050). Total RNA sequencing was processed following a standard Illumina library preparation and sequencing protocol (Illumina Truseq Stranded Total RNA HMR kit, Illumina and Novaseq 6000 S4 v1.5 Reagent kit (300 cycles); RRID: SCR_016387). The repertoire of miRNAs expressed in CICs and FBS cell lines was assessed through the nCounter technology (N = 800 human miRNAs, nanoString, Seattle, WA, USA; RRID: SCR_023912). The transcriptomics characterization of the cell lines was assessed through QuantSeq 3'mRNA-Seq Library Prep Kit-FWD kit (Lexogen, Vienna, Austria). *The details of the genomics* and *bioinformatics methods are described in S4 and S5 sections of Supplemental Materials.*

Functional characterization of miRNAs

qRT-PCR was performed to assess miRNA expression in N = 18 CICs (1247, 1076, 111011, 14583, #2, #3, #5, #7, #8, #9, #11, #13, #14, #16, #20, #21, #57 and #59) and in N = 7 FBS tumor cell lines (1247, 1076, 111011, 1869, 1872, SW480 and SW620). qRT-PCR was performed to assess miRNA expression in CRC (N = 2; CR561147, CR561162) and normal (N = 2; CR559319, CR559504) tissue pairs (Origene). The target genes for the selected miRNAs have been predicted using BRB ArrayTool microRNA targets http://linus.nci.nih.gov/BRB-ArrayTools.html. These results have been integrated with those obtained from other bioinformatics resources, TargetScan; RRID: SCR_010845, miRNAMap; RRID: SCR_003156, MIRDB, miRcancer, OncomiRDB, MiRonTop and MAGIA. The latest two tools allowed the correlation of miRNA and RNA seq data sets. The selected miRNAs were further explored for the regulation of candidate genes in CICs and FBS tumor cells. Briefly, the cell lines were cultured in Opti-MEM™ I Reduced Serum Medium (Thermo Fisher Scientific, Cat # 11058021), in 6-well plates and transfected with 50 nM of either mimics or inhibitors of miR-15a or miR-196a (mirVana kit, Thermo Fisher Scientific, Cat # 4464084) using the NEON transfection kit (Invitrogen, MPK10096K and MPK10096R) according to the manufacturer's instructions. Cells were also transfected with 50 nM of either mirVana miRNA mimic Negative Control #1 (Thermo Fisher Scientific, Cat #4464058,) or mirVana miRNA inhibitor Negative Control #1 (Thermo Fisher Scientific, Cat #4464076,). Following 4 h, the complete medium was then added to the cells, and cells were cultured in vitro for 48 h for further assessments, including qRT-PCR and proliferation assays (see the details in sections S6 and S7 of Supplemental Materials).

Indoleamine 2,3-dioxygenase (IDO) activity in CICs and FBS cell lines

CICs and FBS cell lines were plated in their specific culture media supplemented with 2.5 mM of L-tryptophan (Sigma-Aldrich, Cat #T8941) for 48 h in the presence or not of IFN-γ (1000 U/mL), with or without 2.5 µM (Sigma-Aldrich, Cat #860646) of IDO inhibitor, 1-methyl-DL-tryptophan (1-MT). Supernatants were then collected and treated with 0.2% Trichloroacetic acid (TCA, Sigma-Aldrich, Cat #860646) to precipitate proteins and then, processed to detect the presence of kynurenine. Briefly, an equal volume of p-(Dimethylamino)-benzaldehyde (1.2% in 100% acetic acid) (Sigma-Aldrich, Cat #156477) was added to the supernatant and the detection of kynurenine in the supernatants was subsequently determined using a spectrophotometer at a wavelength

of A_{490} (FLUOstar Omega microplate reader, BMG Labtech, Germany; RRID: SCR_025024). A standard curve of serial dilutions of kynurenine diluted in one part of phosphate buffered saline (PBS), one part 0.2% TCA and two parts 1.2% p-(Dimethylamino)-benzaldehyde in pure acetic acid was performed.

Mixed lymphocyte tumor cell cultures (MLTCs)

CICs and/or FBS cells upon either the modulation of the expression of defined miRNAs (*see above*) or the treatment with immunomodulatory or epigenetic drugs or combinatorial treatments were irradiated (300 Gy) and used to stimulate HLA-A*0201 matched PBMCs from HDs. Briefly, 2×10^5 PBMCs/well were plated in 96 flat-bottom well plates and irradiated (300 Gy) tumor cells at 5:1 lymphocyte/tumor cell ratio, in the presence of IL-7 and IL-15 (10 ng/ml) (Cat #200-07 and Cat #200-15, PeproTech) as previously described [27]. The tumor-specific release of IFN-γ and/or IL-4 by the T cells has been determined through EliSpot assays (Mabtech, Cat #3420-2A or CTL, Immunospot, Cat #hIFN-γIL4-1M; RRID: SCR_011082) following the co-culture of CICs or FBS tumor cells pre-treated or not with either IFN-γ, epigenetic drugs or mimics or inhibitors of selected miRNAs.

In vivo experiments with Zebrafish model

Zebrafish adults were maintained in a 28.5 °C tank at the Zebrafish Facility at Sidra Medicine. At 24 h-post-fertilization (hpf), embryos were transferred to an E3 medium containing 0.2 mmol/L 1-phenyl-2-thio-urea (PTU) to block pigmentation and improve optical transparency of embryos. At 48 hpf, embryos were anesthetized with 0.04 mg/ml of MS-222 (Sigma-Aldrich, Cat #E10521) for CICs xenografts. Primary CICs or FBS cell pair (1247), either un-treated (UT) or pre-treated with modulation of miRNA-15a or –196a (50 nM) in combination or not with Buthyrate (1 mM), were labeled with 2 µg/mL of 1,1'-Dioctadecyl-9 3,3,3',3'-tetramethylindocarbocyanine perchlorate (DIL, Sigma) for emission of red fluorescent signal upon stimulation with UV light. These cells were injected (50 cells/nL) into the perivitelline space of 48 hpf zebrafish embryos (N = 18 embryos for UT CICs, N = 10–12 for miR-15a or miR-196a inhibitor- or mimic-treated tumor cell lines; each experiment was performed two–three times) using a Harvard apparatus microinjector. After injection, xenografted zebrafish larvae were kept in 12-well plates and maintained in a 32 °C incubator along the duration of the experiments. A fluorescence microscope (Cell Discoverer 7, Zeiss) has been used to monitor the localization of tumor cells in the zebrafish larvae. The viability of xenografted zebrafish larvae has been assessed through the monitoring of heart beats, blood circulation, and physical movement. Fluorescent signals were measured through imaging and Zen Blue software (Zeiss) was used to provide quantifications of fluorescence. The behavior and migration of tumor cells in the trunk and tail regions of zebrafish have been monitored.

Statistical analysis of in vitro and in vivo functional assays

Prism software (GraphPad; RRID: SCR_002798) was used for two-tailed paired Student's t-tests for in vitro assays and for two-tails unpaired Student's t-tests for in vivo assays. The p values were $^*p<0.05$, $^{**}p<0.01$, and $^{***}p<0.001$.

Study approval

All animal work and procedures were approved by the Sidra Medicine Institutional Animal Care and Use Committee protocol # SIDRA-2023-001. The animal experiments were performed in accordance with relevant guidelines and regulations.

Results

Multi-omics characterization of CRC-CICs as compared to the bulk tumor cell lines

The comprehensive genomic analysis of CRC-CICs (N = 19) vs. FBS tumor cell lines (N = 7) was achieved through the assessment of the methylation of genes and promoters, total RNA sequencing and the profiling of N = 800 miRNAs.

Gene expression

A differential gene expression profile was detected in CICs vs. FBS tumor cells. Box plot showing the Log2 CPM (counts per million) of normalized RNA sequencing data for each cell type, with CICs represented in red and FBS in blue, is represented in Figure S1A. The Principal Component Analyses (PCA) for gene expression (GE) showed the different spatial distribution of the two subtypes of cells (Fig. 1A). Overall, N = 1187 genes were detected out of a total of N = 15,913 with measured expression, as differentially expressed with $p<0.05$ (*data not shown*). Through applying the threshold of $p<0.01$ and logarithmic fold change (LogFC) of 1.5, N = 132 genes resulted as significantly differentially expressed in CICs as compared to FBS tumor cells (Table S4). The graphical representation of the results is shown in the volcano plot and heatmap in Fig. 1B–C, respectively. These data were analyzed in the context of Gene Set Enrichment Analyses (GSEA), Gene Ontology (GO) annotation and pathways enrichment using iPathwayGuide (Advaita Bioinformatic). In summary, 33 pathways were found to be significantly impacted (Table S5) highlighting the hub function of differentially expressed genes (DEGs) (N = 40) and significant pathways (N = 26)

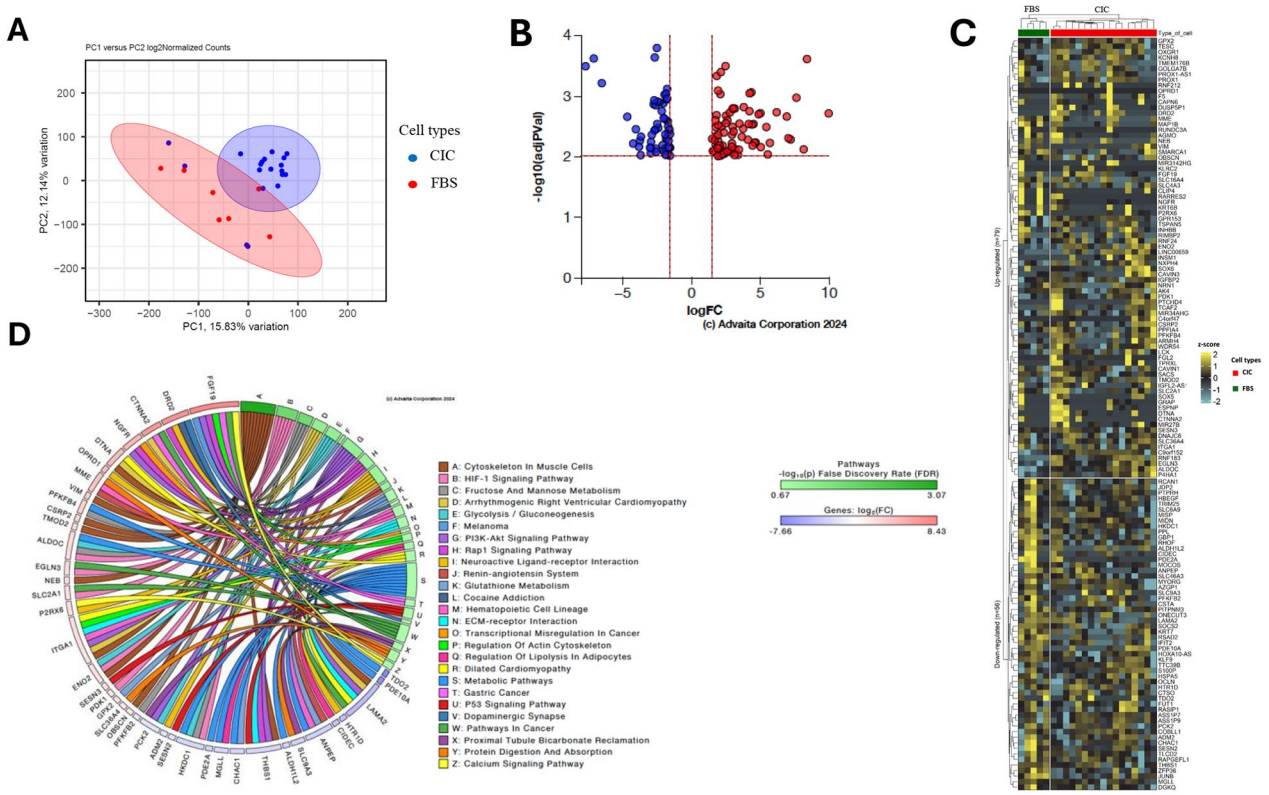

Fig. 1 Differential gene expression and biological pathways detected in CRC-CICs vs. -differentiated tumor cells. A comprehensive genomic analysis of CRC-CICs (N = 19) vs. differentiated bulk tumor cell lines (n = 7) was achieved through total RNA sequencing (Novaseq 6000, Illumina) (for further details, *see sections S4.2 and S5 of Supplementary Materials and Methods*). **A** Principal component analysis (PCA) plot shows the expression variability of genes dimensionally reduced to sample type, CICs (*blue dot*) and differentiated tumor cells (*red dot*), leading to distinct cluster formation. The percentage of total variation accounted for the 1st (15.83%) and 2nd (12.14%) principal components are shown on the x and y axes, respectively, demonstrating a clear spatial separation between CICs and FBS tumor cells. **B** Volcano plot of N = 132 differentially expressed genes (LogFC 1.5 and $p < 0.01$) in CICs vs. differentiated tumor cells, showing a differential gene distribution between both cell populations. The vertical red lines refer to a 1.5-fold (log10 scaled) up-regulation and down-regulation, respectively. The horizontal red line corresponds to a *p*-value of 0.01. **C** Annotation heatmap showing the expression distribution of top 132 up and downregulated DEGs in CRC-CICs vs. FBS tumor cells. Cluster dendrograms representing Euclidean distance-based hierarchical clustering for both rows and columns are presented along the *left* and *top* sides of the plot. Sample type (*red* for CICs and *green* for differentiated tumor cells) are presented at the top of the heatmap. The location of each gene on its respective chromosome number is presented in the right panel. Z-score normalization was performed on the normalized read counts associated with each gene sample. CICs displayed clear differential clusters of genes compared to FBS tumor cells. **D** Chord plot showing the relation of 40 hub DEGs (on *right semicircle track*) with 26 significant pathways (on *left semicircle track*, named by letters) via colored edges. The edges initiate from unique colored strips present on the right semicircle (indicating genes) and converge to unique colored strips present on the left semicircle (indicating pathways; *see the side legend*). Many molecular pathways were significantly upregulated in CICs, including cytoskeleton and migration, HIF-1, fructose and mannose metabolism, glycolysis/gluconeogenesis, EMT and TGF-β

($p < 0.05$; shown via colored edges in the chord plot of Fig. 1D). In addition, N = 877 Gene Ontology (GO) terms and N = 67 gene upstream regulators, were found to be significantly enriched before the correction for multiple comparisons. The top significantly detected molecular pathways included: (i) the cytoskeleton in muscle cells (KEGG04820) (FDR $p < 8.490e{-}4$), including the perturbation of genes involved in desmosome, focal adhesion, dystroglycan complex (*DGC*) and spectrin based membrane cytoskeleton and sarcomere (Figure S2A). (ii) The hypoxia-inducible factor 1 (HIF-1) signaling pathway (false discovery rate, FDR $p < 0.02$), which acts as a master regulator of numerous genes inducible by hypoxic conditions, and, additionally, by nitric oxide and growth factors. N = 6 genes from HIF-1 pathway were found to be differentially modulated in CICs vs. FBS cell lines including aldolase, fructose-bisphosphate C (*ALDOC),* Egl-9 Family Hypoxia Inducible Factor 3 (EGLN3*),* Enolase 2 *(ENO2),* hexokinase domain component 1 *(HKDC1),* Pyruvate Dehydrogenase Kinase 1 *(PDK1)* and Solute Carrier Family 2 Member 1 *(SLC2A1)* (Figure S2B). Other differentially expressed pathways were (iii) the

fructose and mannose metabolism, glycolysis/gluconeogenesis and, although with less stringent p value, and (iv) the PI3K/Akt1 signaling, with N = 6 perturbated genes, Fibroblast growth factor 19 (*FGF19),* Nerve Growth Factor Receptor *(NGFR),* Integrin Subunit Alpha 1 *(ITGA1)* (upregulated) and Laminin Subunit Apha 2 (*LAMA2),* TGF-β signaling with the thrombospondin 1 *(THBS1), an* activator of TGF-β/smad2/3 signaling which promotes invasion, cancer progression and facilitates EMT [28, 29], and Phosphoenolpyruvate Carboxykinase 2, Mitochondrial (*PCK2)* (downregulated) (Figure S2C–E). Moreover, the antigen processing and presentation pathway was indeed detected with killer cell lectin like receptor C2 (*KLRC2*) being upregulated, the Heat Shock Protein Family A (Hsp70) Member 5 (*HSPA5)* and *THBS1* being downregulated (Figure S2F), as well as the inhibin subunit beta B (*INHBB) being* upregulated (Figure S2G). Among other pathways that were differentially detected between CICs and FBS tumor cells are p53, mTOR and TNF signaling via NF-κB pathways (Table S5). The list of differentially expressed genes is provided in Table S4 that includes genes related to cancer development and progression, e.g., the unfolded protein response component Cation transport regulator homolog 1 (*CHAC1*) [29], *HKDC1* which promotes tumor immune evasion in hepatocellular carcinoma by coupling cytoskeleton to STAT1 activation and programmed cel death ligand 1 (*PD-L1*) [30]. Moreover, *ALDOC*, that is also involved in tumor cell spheroid formation, was 2.5-fold upregulated in CICs compared to FBS tumor cells [31] while the lymphocyte-specific protein tyrosine kinase (*LCK*), implicated in various oncogenic processes, particularly in CRC [32], was fivefold upregulated in CICs. On the other hand, JUN B proto-oncogene (*JUNB*), a direct target of TGF-β-Smad signaling, which can act as tumor suppressor or oncogene depending on the cancer entity [33, 34], was found to be downmodulated in CRC-CICs vs. FBS tumor cell lines.

Analysis of the differentially methylated regions (DMR) in CRC-CICs compared to FBS tumor cells

Following the data quality control and normalization, a total of 3529 differentially methylated sites were identified. A combined rank among the 500 best ranking regions was applied to identify differentially methylated genes (n = 79) and promoters (n = 31) in CRC-CICs vs. FBS cell lines. N = 48 and 31 genes were either hypomethylated or hypermethylated, respectively while, at the promoter levels, N = 9 and 22 were hypomethylated and hypermethylated, respectively in CRC-CICs as compared to FBS cell lines (p-value ≤ 0.11; Figure S3). The GO enrichment analysis was conducted for the gene and promoter's regions using the GOseq R program and an adjusted p value of <0.05 was set as cutoff. A total of N = 63 hypermethylated and 44 hypomethylated biological processes (BP) were enriched in the gene regions. The functional enrichment of hypermethylated genes in BP includes macromolecule and cellular localization and the obsolete regulation of canonical Wnt-signaling pathways. In terms of promoters, N = 77 and 65 hypermethylated and hypomethylated BPs, respectively were enriched. The top list included the cardiac muscle cell fate commitment, animal organ morphogenesis, cell development and regulation of multicellular organism development. Of note, BPs involved in the regulation of miRNAs were also identified. Table 1 shows the results of shared genes and biological processes between DNA methylation and total RNA-seq data that were differentially detected in CICs vs. FBS tumor cells, including animal organ development and regulation of immune system pathways (Table 1a), *JUNB*, and *THBS1*. BPs for hypermethylated promoters are cell development, multicellular organismal development and L-tryptophan transmembrane transport (Table 1c). Among the numerous BPs detected in the hypomethylated regions upon the integration of DEGs (Table 1d) are the activation of immune response and immune response-regulating cell surface receptor signaling pathways. Of interest, both *LCK*, which plays a role in cell cycle control, cell adhesion, motility, proliferation and differentiation, and *KLRC2*, which regulates mechanisms of antigen presentation and antitumor activity belong to the pathways mentioned above.

MiRNA profiling

The class comparison of the profile of miRNAs in CRC-CICs vs. FBS tumor cells led to the identification of N = 57 differentially expressed miRNAs ($p \leq 0.05$). PCA depicted a clustering of CICsvs. differentiated cell lines. PC1 and PC2 explained 48.42 and 11.26% of the variability in the expression data, respectively (Figure S1B). Figure 2A shows the heatmap of differentially expressed miRNAs between CICs and FBS tumor cells. Most of the miRNAs were found to be upregulated in CICs vs. FBS cell lines, including the N = 11 top scored differentially expressed ($p < 0.02$, miRNAs -299, -15a, -210, -196a, -362, -378d, -3144, -4461, -4488 and let-7d). Ingenuity Pathway Analysis (Qiagen) was performed to determine either the computationally predicted or the experimentally validated target genes for the miRNAs, showing their involvement in tumorigenic functions, such as cell cycle, migration, development and proliferation and the regulation of EMT (Fig. 2B). KEGG pathways associated with these miRNAs (Fig. 2C) included the mTOR, PI3K/Akt1, p53 and TGF-β signaling that represented also the top pathways related to the differentially expressed genes (DEGs) in CICs vs. FBS tumor cells (Table S5).

Table 1 Biological pathways and their related genes detected through the integration of the data sets from differential DNA methylation and RNA sequencing of CRC-CICs vs. -FBS tumor cells

Shared GO*	Shared genes	LogFC[#]
(a) *Hypermethylated genes*		
Animal organ development	PCK2	−1.7338538
	MYORG	−1.7574485
	CSTA	−6.4784441
	PROX1-AS1	3.4852361
	PPL	−1.5247145
	NGFR	5.04380677
	RCAN1	−2.0037422
	MME	4.2610101
	JUNB	−1.6613906
	SLC2A1	2.21755586
	SMARCA1	1.7958435
	INSM1	4.38601726
	KRT7	−1.808263
	SOX6	2.39366782
	TMEM176B	2.54434731
	LAMA2	−4.2012489
	HBEGF	−2.5415349
	FGF19	8.42612971
	DRD2	7.65804354
	VIM	3.78839954
	INHBB	2.54830042
	NEB	2.30409572
	FUT1	−1.5296596
	PDE2A	−2.5343748
	RARRES2	4.91174051
	SOX5	7.07552558
	HSPA5	−1.7664794
	SOCS2	−2.4551316
	KRT6B	10
	CTNNA2	7.23660646
Regulation of immune system process	FGL2	3.83356598
	KLRC2	6.95888723
	ZFP36	−2.060365
	LCK	5.4723652
	DRD2	7.65804354
	IGFBP2	2.82439579
	RARRES2	4.91174051
	JUNB	−1.6613906
	GBP1	−4.6265957
	THBS1	−2.710031
	RSAD2	−3.6514069
	RSAD2	−3.6514069
	TRIM25	−1.8108806
	TMEM176B	2.54434731
(b) *Hypomethylated genes*		
Negative regulation of epithelial cell proliferation	NGFR	5.04380677
	DRD2	7.65804354
	KLF9	−3.7130774
(c) *Hypermethylated promoters*		
Cell development	MYORG	−1.7574485
	PROX1-AS1	3.4852361

Table 1 (continued)

Shared GO*	Shared genes	LogFC#
	NGFR	5.04380677
	CTNNA2	7.23660646
	LAMA2	−4.2012489
	ZFP36	−2.060365
	RCAN1	−2.0037422
	TMOD2	2.64965106
	NRN1	2.04161851
	INSM1	4.38601726
	ITGA1	2.13034481
	OBSCN	1.5996479
	CSRP2	3.01137124
	DRD2	7.65804354
	VIM	3.78839954
	INHBB	2.54830042
	NEB	2.30409572
	PDE2A	−2.5343748
	JUNB	−1.6613906
	MAP1B	2.97615097
Regulation of multicellular organismal development	FGL2	3.83356598
	LAMA2	−4.2012489
	PROX1-AS1	3.4852361
	ZFP36	−2.060365
	NGFR	5.04380677
	DRD2	7.65804354
	MME	4.2610101
	FUT1	−1.5296596
	ADM2	−1.7340464
	SOX5	7.07552558
	JUNB	−1.6613906
	THBS1	−2.710031
	SOX6	2.39366782
	MAP1B	2.97615097
	TESC	2.93902607
	TMEM176B	2.54434731
L-Tryptophan transmembrane transport	SLC36A4	1.61661777
(d) *Hypomethylated promoters*		
Activation of immune response	KLRC2	6.95888723
	LCK	5.4723652
	TRIM25	−1.8108806
Negative regulation of proteolysis	CSTA	−6.4784441
	CHAC1	−2.6302142
Intrinsic apoptotic signaling pathway	PDK1	1.87335134
	CHAC1	−2.6302142
Immune response-regulating cell surface receptor signaling pathway	LCK	5.4723652
	KLRC2	6.95888723

A comprehensive genomic analysis of CRC-CICs (N = 19) vs. -differentiated (FBS) bulk tumor cell lines (n = 7) was achieved through the assessment of the methylation of genes and promoters (Infinium Methylation EPIC V.1 BeadChip, Illumina) and total RNA sequencing (Novaseq 6000, Illumina) (for details, *see sections S4 and S5 of Supplemental Materials*). Differential gene expression profile was detected in CICs vs. FBS cell lines, including few autologous pairs ($p \leq 0.01$, logFC > 1.5). For DNA methylation analysis, the Gene ontology (GO) Enrichment Analysis was conducted using a hypergeometric test that addresses the hierarchical structure of the ontology and a combined rank among the 500 best ranking regions was applied followed by setting cutoffs of an adjusted p value < 0.05 to identify differentially methylated genes and promoters ($p < 0.05$). The biological processes (BP) and DEGs obtained by the integration of both data (DEGs and hypermethylated (a), hypomethylated (b) genes, hypermethylated (c) and hypomethylated (d) promoters, sets are represented in the Table. *Gene ontology biological processes, #Log Fold change

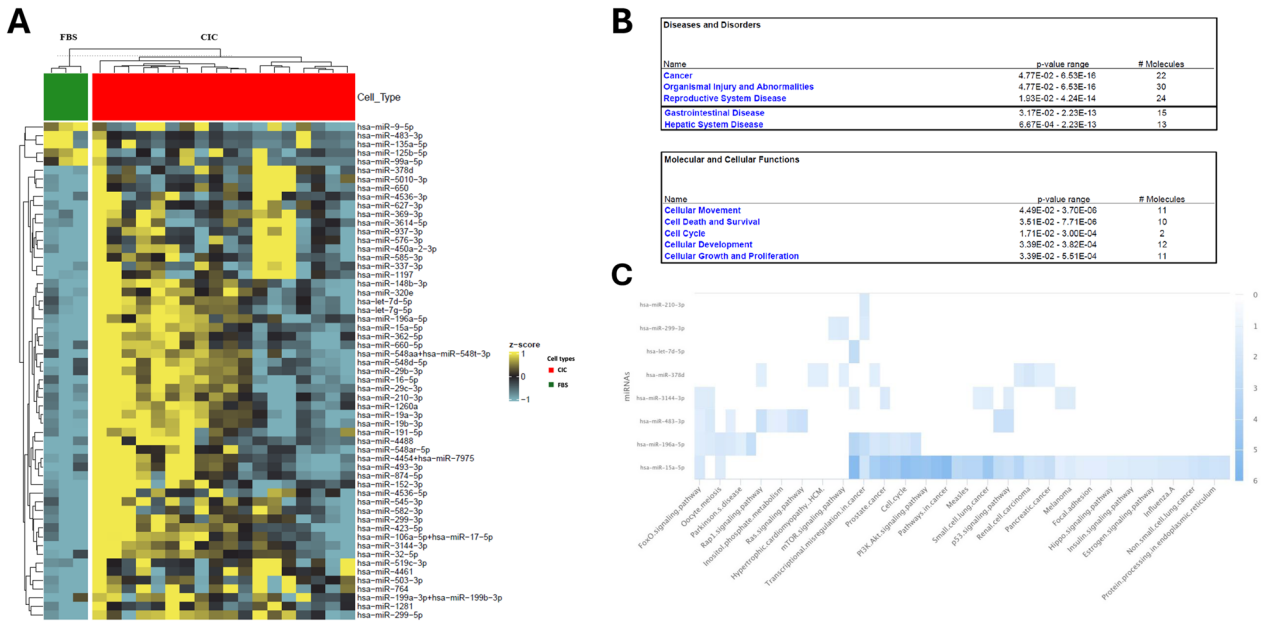

Fig. 2 Differential expression of miRNAs in CRC-CICs vs. -differentiated tumor cells. miRNA profiling was performed in CRC-CICs (n = 19) vs. -differentiated (FBS) tumor cells (n = 3) using the nCounter technology (nanoString) to detect the expression of N = 800 human miRNAs. The bioinformatics analyses were performed with R packages and ANOVA statistical analysis ($p < 0.05$) (for details, *see sections S4.3 and S5 of Supplemental Materials and Methods)*. The pathway analysis was performed using Ingenuity pathway analysis (Qiagen). **A** Annotation heatmap showing the distribution of differentially expressed (N = 57; $p \leq 0.05$) miRNA in CRC-CICs (*red bar*) vs. differentiated tumor cells (*green bar*). Cluster dendrograms representing Euclidean distance-based hierarchical clustering for both rows and columns are presented along the *left* and *top* sides of the plot. Most of the miRNAs were found to be up-regulated in CICs vs. FBS cell lines and a clear distinction in the miRNA profile signature was found between these subsets of tumor cells. **B** Functional Interpretation and pathway analysis of the identified N = 57 differentially expressed miRNAs showing the involvement of upregulated miRNAs, found in CRC-CICs, in tumorigenic functions, such as cell cycle, migration, development and proliferation and the regulation of EMT. **C** Top KEGG pathways of the N = 11 top differentially expressed miRNAs ($p < 0.02$). Top differential KEGG pathways included the mTOR, PI3K/Akt1, p53 and TGF-β signaling. The bioinformatics analyses were performed with R packages and ANOVA statistical analysis ($p < 0.05$)

The comparison of data sets from DNA methylation and miRNA profiling showed that miR-15a and miRNA-196a could target mRNAs transcribed from hypomethylated genes and promoters (Table S8). Other miRNAs that were upregulated in CICs and linked to hypomethylation were miRNA-16, tightly linked to miRNA-15a, and let-7g. Interestingly, only miRNA-125b and -483 were among those downregulated in both data sets (hypermethylated genes and promoters and miRNA profiling) (Tables S7 and S8).

Functional validation of the modulation of miRNAs in CICs vs. differentiated cells

The upregulation of miRNA expression, except for miR-4461, in CICs (N = 18) as compared to FBS tumor cells (N = 9) (Fig. 3A) was assessed through qRT-PCR. MiRNAs-15a and -196a were statistically significantly up-regulated (20-fold, $p \leq 0.01$ and twofold, $p \leq 0.05$, respectively) in CICs. However, it is important to note that these miRNAs are downmodulated in CRC vs. distant normal mucosal pair tissues (Figure S4). This information was considered when exploring the functional role of these miRNAs, comparing the effect of both inhibition and mimics. The computationally predicted target genes of these miRNAs were compared with DEGs data and the genes regulated by both miRNA -15a and -196a were selected for further functional validation, focusing on immune functions, EMT and stemness. Using the ingenuity pathway analysis (IPA) software, the cellular network of miR-15a and miR-196a with molecular pathways, detected through DEG analyses, were identified (Figure S5). These include TGF-β, PI3K/AKT, actin cytoskeleton signaling and PD-1, PD-L1 cancer immunotherapy, for which the principal involved genes are *CRK* Like Proto-Oncogene (*CRKL*) [35], AKT Serine/Threonine Kinase 1 (*AKT3), CD274 (PD-L1),* Transforming Growth Factor Beta Receptor 2 (*TGFBR2),* SMAD family member 3 (*SMAD3)* and *JUNB* (Figure S5).

The modulation of miRNAs -15a and -196a by transient transfection with mimics was investigated in cell line pairs (#1076 and #1247) showing 15-, 20-, 12- and 12.5-fold upregulation of miRNA-196a and miRNA-15a

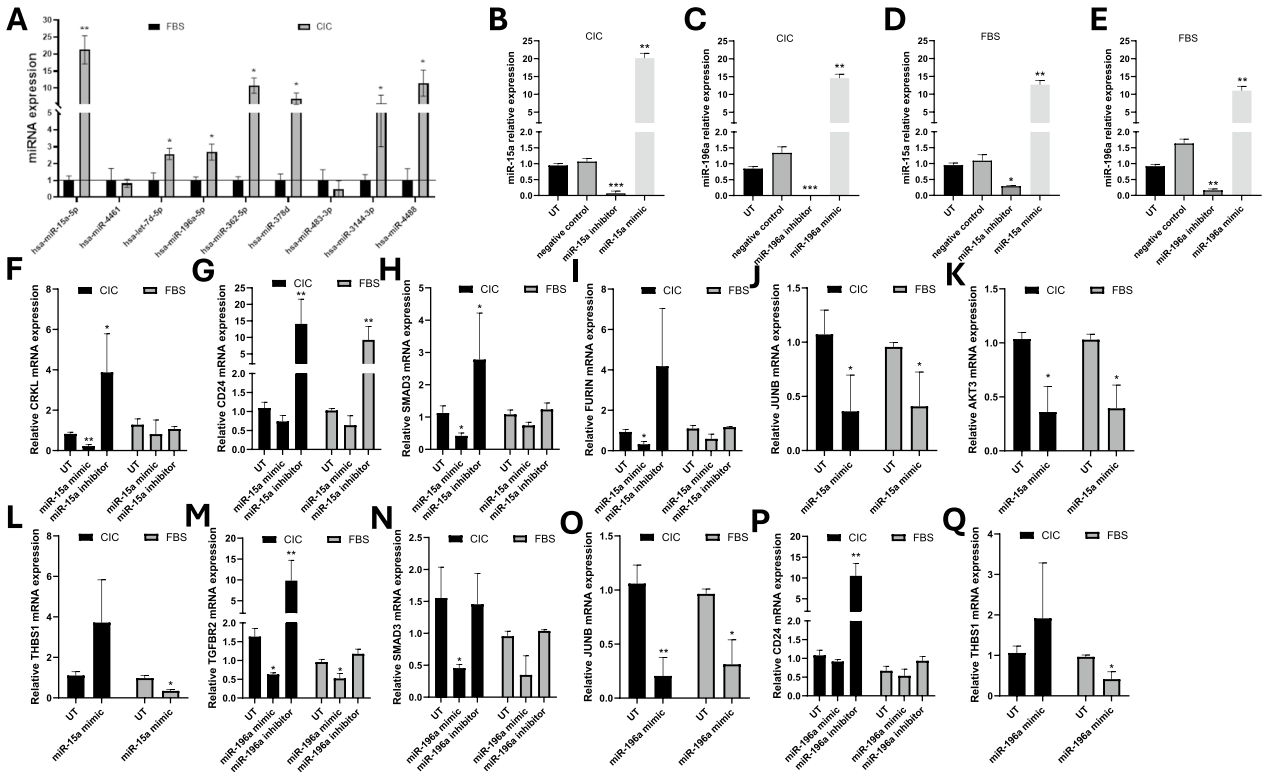

Fig. 3 Expression of selected of miRNAs, their modulation and modification of the expression of the target genes. The expression of the following miRNAs: -15a, -196a, -362, -378d, -483, -3144, -4461, -4488 and let-7d, was assessed by qRT-PCR in CICs (N = 18) vs. FBS (N = 7) cell lines; **A** *black* and *grey bars* represent miRNA expression in CICs and FBS cell lines, respectively. **B**–**E** represent the modulation of the expression of miRNAs −15a and −196a in 1247 and 1076 CICs (Panels **B** and **C**) and differentiated tumor cells (**D**, **E**) following the transfection with 50 nM of either mimics or inhibitors of these miRNAs. The detection, through qRT-PCR, and the modulation of the predicted target genes upon transfection with either miR-15a (CRKL, CD24, SMAD3, FURIN [36], JUNB, AKT3 and THBS1, **F**–**L**) or miRNA-196a (TGFBR2, SMAD3, JUNB, CD24 and THBS1; **M**–**Q**) modulators was assessed, by qRT-PCR in 1247 and 1076 CRC cell line pairs. Means ± SD values from three experiments are shown. *$p < 0.05$, **$p < 0.01$, ***$p < 0.001$

in CICs or FBS tumor cells, respectively (Fig. 3B–E). On the other hand, the inhibitors of the same miRNAs led to complete gene silencing in CICs (Fig. 3B, C) or FBS tumor cell lines (Fig. 3D, F). The treatment of CICs with miRNA-15a mimics resulted in a significant decrease in the expression of the predicted target genes *CRKL*, *FURIN* [37], *SMAD3*, *JUNB* and *AKT3 (*fivefold, $p < 0.01$ and 3-, 2.8-,3.2- and threefold, $p < 0.05$, respectively) (Fig. 3F, H–K) implicated in either EMT progression or CIC phenotype, including the regulation of the stemness markers LGR5 and NANOG) [36]. Similar, although weaker, effect was observed in FBS cell lines. On the contrary, *THBS1* was found as up-regulated in the CICs (threefold, $p < 0.05$, respectively) (Fig. 3L). The inhibition of miRNA-15a in both CICs and FBS cell lines (1.4- and 1.6-fold, respectively) resulted in a significant ($p < 0.05$) up-regulation, with superior effect in CICs, of the target genes mentioned above (Fig. 3F–I). MiR-196a overexpression in both CICs and FBS cell lines resulted in the specific downregulation of *TGFBR2, SMAD3* and *JUNB* mRNAs with the exception of *THBS1* whose modulation was observed only in FBS cell lines (2–5.2-fold, and 2–3-fold in CICs and FBS tumor cell lines, respectively; $p < 0.05$) (Fig. 3M–O, Q). The inhibition of miR-196a increased the expression of same genes (Fig. 3 M–O, Q). Weak and not statistically significant decrease of the expression of CD24 mRNA was detected upon the mimicry with both miRNA-15a and miRNA-196a (Fig. 3G, P).

Distinct response to immunoregulation, epigenetic drugs or miRNA-15a between primary CRC-CICs and differentiated cell lines

We next investigated the ability of either IFN-γ (Fig. 4C, D) or of epigenetic agents 5-aza, RG108 (Fig. 4E, F), HDACi (Vorinostat) or or the regulator of HDAC Sodium Butyrate (Butyrate) (Fig. 4G, H) to increase the expression of MHC class I, class II and APM molecules (HLA class I, class II, ICAM-1, β2-microglobulin (β-2m), TAP-1,2, LMP-2,7,10, Tapasin, Calnexin and Calreticulin) (Fig. 4A, B) which were previously reported as commonly

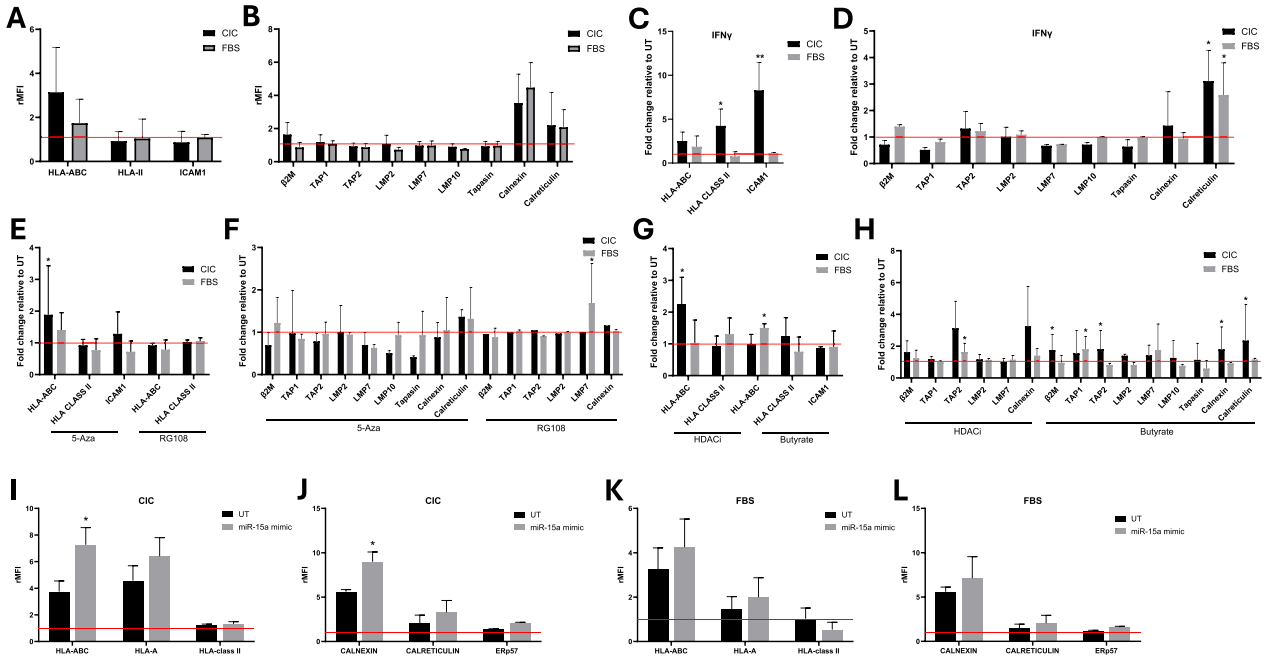

Fig. 4 Expression of HLA and APM molecules in CRC-CICs and FBS tumor cells following or not the treatment of the cells with epigenetic or immunomodulatory agents. The assessment of the expression of HLA (HLA-ABC, HLA-Class II, ICAM1; **A**) and APM (β2-microglobulin, Calnexin, Calreticulin LMP2, LMP7, LMP10, TAP1, TAP2 and Tapasin; **B**) markers was performed through flow cytometry in primary CRC-CSCs (N = 6) and FBS tumor cell lines (N = 3). Cell lines were treated or not (UT, **A**, **B**) with either 1000 IU/mL IFN-γ for 48 h (**C**, **D**) or 5 μM of 5-Azacytidine (5-Aza) or 5 μM of RG108 (**E**, **F**) or for HDACi (1.25 μM Vorinostat + 0.3 μM Mithramycin A) for 24 h or overnight with 1 mM Buthyrate (**G**, **H**). The primary CRC-CSCs (N = 3, **I**, **J**) and differentiated pair cell lines (N = 3; **K**, **L**) were transfected for 48 h with miR-15a mimics and then the expression of HLA-ABC, HLA-A, HLA-Class, Calnexin, Calreticulin and ErP57 molecules was assessed by flow cytometry. Data in the Figure are represented as relative mean of intensity of fluorescence (rMFI) calculated for each marker as the ratio of the mean of intensity of fluorescence between the stained and unstained samples. Means ± SD values from three experiments are shown. *$p < 0.05$, **$p < 0.01$

down-modulated [14]. The pre-incubation of tumor cells for 48 h with IFN-γ (1000 IU/mL) could, markedly, increase the expression of HLA-class I, HLA-class II and ICAM-1 (2-, 4- and eightfold, $p < 0.05$) in CRC-CICs, whereas no effect was observed for FBS tumor cell lines (Fig. 4C, D). Among the APM molecules, only calreticulin was significantly upregulated by IFN-γ in both CICs and FBS cell lines (Fig. 4D). The treatment of these cell lines with the demethylating agents 5-aza and RG108 did not substantially improve the overall expression of HLA and APM molecules, with only a weak increase of HLA-class I and calreticulin (5-Aza; 1.4-, 1.8-fold, $p < 0.05$) (Fig. 4E, F). Vorinostat or Butyrate increased the levels of HLA-class I (2.2-fold, $p < 0.05$ by Vorinostat), β-2m, TAP-2, Calnexin and Calreticulin (1.76-, 1.81-, 1.8- and 2.4-fold, respectively, $p < 0.05$ by Buthyrate) on CICs (Fig. 4G, H). These results showed that the treatment of tumor cells with immunomodulatory or epigenetic agents can increase the expression of some, but not all, the molecules involved in antigen processing and presentation of CRC cells, with distinct effect between the two types of cancer cell lines, which may be insufficient to elicit an efficient tumor-specific T cell recognition.

The transfection of CRC-CICs with miRNA-15a mimics led to the significant up-regulation of HLA-I and Calnexin (1.9- and 1.6-fold, respectively, $p < 0.05$), at superior levels as compared to HDACi or Butyrate, while the expression of HLA-A, Erp5 and Calreticulin was upregulated but without statistical significance (Fig. 4I, J). Weaker effect, without statistical significance, on the same molecules was observed in FBS tumor cell lines (Fig. 4K, L).

Taken together, these results suggest that the up-regulation of the expression of miRNA-15a can rescue the immunogenicity of CICs, with, in some cases, superior effect as compared to epigenetic agents.

MiRNA modulation or epigenetic drugs can shape the genetic program of CRC cell lines

DEGs were assessed in CICs and FBS cell line pairs (#1076 and 1247) upon treatment with either miRNA-15a or -196a modulators (inhibitors or mimics), immunomodulatory or epigenetic agents (HDACi, Butyrate or IFN-γ + Butyrate). Numerous DEGs were detected through the comparisons of the different treatments. In CICs, N = 176, 238, 131, 168, 1155, 1237 and 1368 DEGs

were significantly ($p < 0.05$) detected following their treatment with either miRNA-15a or miRNA-196a mimics or inhibitors, Butyrate, HDACi or IFN-γ + Butyrate (Figure S6). N = 179, 212, 186, 183, 868, 2228 and 1065 DEGs were significantly ($p < 0.05$) detected following the same treatments of FBS tumor cells (Figure S6). Limited number of matched genes were perturbated in both CICs and FBS tumor cells by either miRNA-15a or miRNA-196a mimics or inhibitors (N = 34, 37, 32 and 35, respectively; Figure S6A–D). The treatments of the cell lines with HDACi or with the combination of IFN-γ plus Butyrate led to a broader effect in terms of the gene regulation (N = 1000 and 598 of genes, Panels F–G). The comparisons of the effect of HDACi, Butyrate or IFN-γ plus Butyrate led to the identification of high numbers of DEGs shared by CICs or FBS tumor cells (Figure S6H-I), suggesting that miRNA-15a or -196a can play also a differential effect on CICs vs. FBS tumor cells that is observed at lower extent for epigenetic agents. Limited shared DEGs were detected in CICs by overlapping the data sets generatedwith different treatments (N = 20 and 30 DEGs, respectively; Figure S6K-L).

The treatment of CRC-CICs or -FBS cell lines with miRNA-15a or miRNA-196a mimics resulted in the overexpression (37.7- and 36.8-fold, respectively) of genes involved in tumor suppression. Of note, one of these genes, Mucin 17 (*MUC17*) [38] was up-regulated preferentially in CICs upon the treatment with either both miRNAs or epigenetic agents or IFN-γ plus Butyrate (38.1- and 39.8-fold change, respectively; Table S9). A novel lncRNA *SOX2-OT*, implicated in tumor progression [39], was detected as downmodulated only in CICs by either the mimics of miRNA-15a or miRNA-196a, or the treatment with Butyrate or IFN-γ plus Butyrate (fivefold to sixfold change) (Table S9). The levels of *THBS1* gene were increased in CICs or FBS tumor cells (2.1- and 2.2-fold change, respectively) by the miRNA mimics, as confirmed by qRT-PCR results (Fig. 3M, R). Many other genes related to TGF-β signaling, such as *TGFB3, TGFBR2* and *TGFBRAP1*, were downregulated by either miRNA-15a, miRNA-196a mimics or Butyrate (Table S9). The modulation of the genes encoding for HLA-A, B, C and APM (β2M) was also observed in CICs upon the over-expression of both miRNA-15a and miRNA-196a, although the values did not reach the threshold of statistical significance ($p < 0.05$) (*data not shown*). Nevertheless, significant up-regulation of these molecules was detected by flow cytometry (*see paragraph 3.3*). On the other hand, the culture in vitro of the CRC cell lines with IFN-γ plus Butyrate led to a statistically significant increase of the levels of transcripts of multiple genes involved in the mechanisms of antigen processing and presentation, such as *HLA-A, B, C, DMB, DRA, DRB1, ICAM1, ICAM5, β2M* in both CICs and FBS tumor cells. However, important molecules for immunogenic functions, such as *TAP2* and *IFNGR1,* were modulated only in CICs (Table S9). The genes encoding for the ligands of the activatory/costimulatory natural killer group 2 member D (*NKG2D*) receptor on NK and T cells (*ULBP-2* and/or *MIC-B)* were modulated (threefold and fourfold change) by Butyrate either alone or in combination with IFN-γ (Table S9). *HLA-E* and *HLA-F*, which are involved in immune evasion mechanisms, were also modulated by these treatments while PD-L1 (CD274) was up-regulated by the combination of IFN-γ plus Butyrate but not by Butyrate alone (Table S9). Notably, HDACi could negatively regulate genes involved in TGF-β pathway, such as *TGFBR2, TGFBRAP, SMAD1,3,4*, and the proto-oncogene *CRKL,* similarly to the effect of the mimic of miRNA-15a and -196a (Fig. 3).

These results corroborate the role of miRNA-15a and miRNA-196a mimics in regulating both the immunogenicity, such as through the downmodulation of TGF-β signaling and the upregulation of HLA and APM molecules, and tumorigenic pathways of CRC-CICs. In addition, epigenetic drugs can represent complementary beneficial treatments.

Increased susceptibility of CICs to T cells upon miRNA modulation and/or the treatment in vitro with epigenetic drugs

PBMCs isolated from HLA class I matched healthy donors (N = 3) were co-cultured (mixed lymphocyte tumor cell cultures; MLTCs) in vitro with CICs (#1247), following the pre-treatment or not of cancer cells with IFN-γ, Vorinostat, 5-aza or butyrate. The anti-tumor reactivity of T lymphocytes was determined through IFN-γ release (EliSpot assay). When CICs were used as antigen presenting cells, a failure in inducing anti-CIC specific T lymphocytes was observed (Fig. 5A), even upon pretreatment of target cells (CICs) with immunomodulatory or epigenetic drugs. Only the HLA-matched FBS tumor cells were recognized by T cells (N = 108 spots/5×10^4 T cells; Fig. 5A). Upon the stimulation in vitro of PBMCs with CICs pre-treated with IFN-γ, an augmentation of the efficiency of T cell reactivity was observed, but only upon the pre-treatment of the target cells with IFN-γ or HDACi (Vorinostat or Butyrate) (N = 19, 23 and 70 spots/5×10^4 T cells, respectively, Fig. 5B). Superior anti-CIC reactivity was observed following the activation of the lymphocytes with cancer cells pre-treated with either Vorinostat, 5-aza or Butyrate and, in the effector phase, the usage of target cells pre-incubated with 5-aza (N = 23, 31 and 50 spots /5×10^4 T cells, respectively; Fig. 5C-E). Consistently with these results, HLA-I, ICAM-1 and Calreticulin were significantly upregulated by 5-aza while

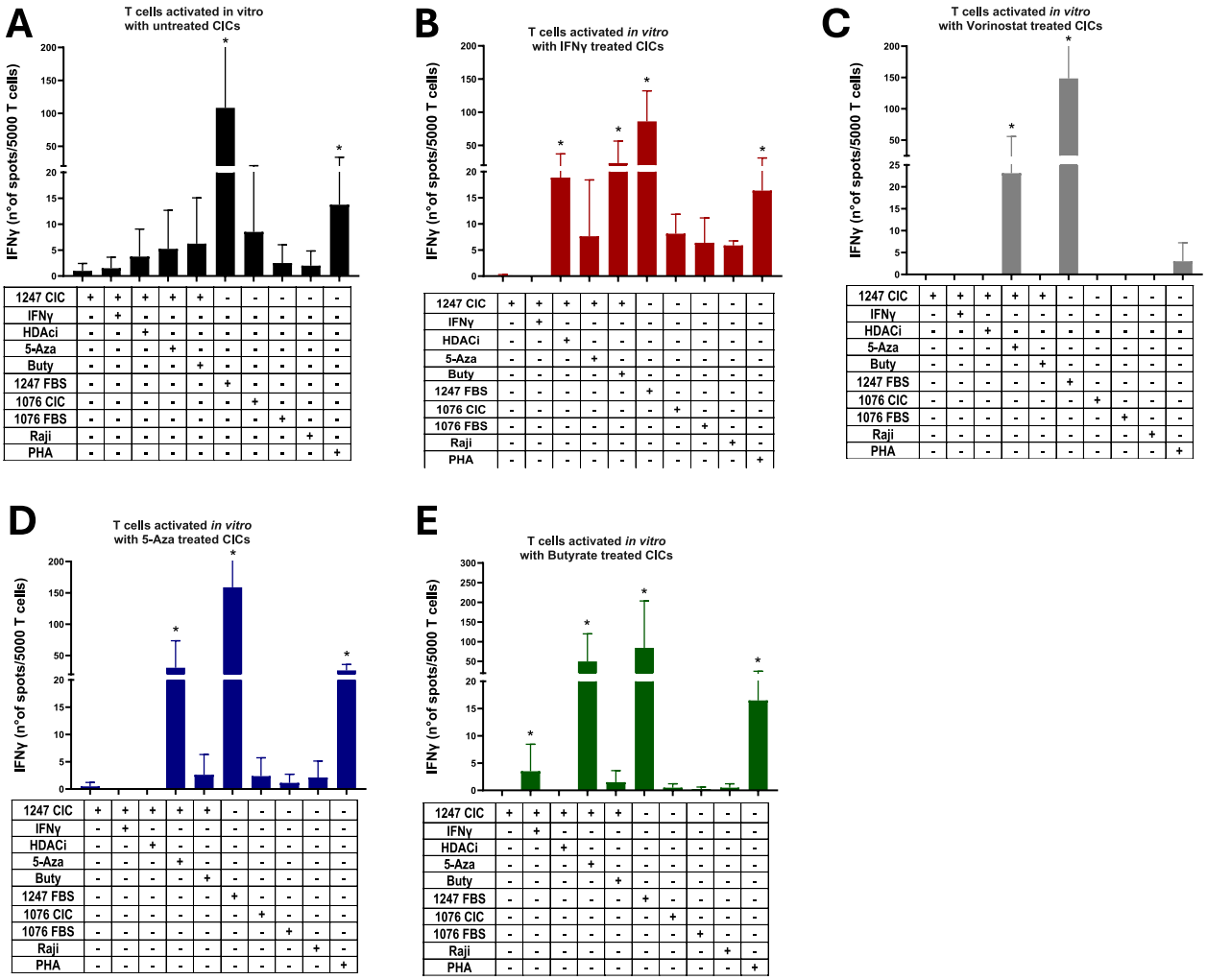

Fig. 5 T cell activation by CICs treated with immunomodulatory or epigenetic agents. PBMCs from HLA class I-matched healthy donors (HD, N = 3) were cultured in vitro with irradiated CRC-CICs with or without (untreated, **A**) pre-treatment of the tumor cells with IFN-γ (48 h) (**B**) or epigenetic agents (24 h): Vorinostat (HDACi, **C**), 5-Azacytidine (5-Aza; Panel D) or Buthyrate (Buty) (**E**). T cells were stimulated bi-weekly with tumor cells. Following 4 weeks of in vitro culture, the tumor-specific release of IFN-γ by T cells was determined by EliSpot assay. T cells were incubated overnight with CICs either untreated or pre-treated with IFN-γ, HDACi, 5-Aza or Buthyrate. The FBS tumor cells (#1247 FBS) were also used as target cells. The HLA mismatched cell lines 1076 CSC and 1076 FBS and the histologically unrelated Raji cell lines were used as controls for antigen-specific reactivity. PHA was added to the T cell cultures as positive control of cytokine release. Data were acquired with the ImmunoSpot analyzer Ultimate V6 (CTL). In the Figure, the means of three experiments are shown. Data are expressed as N. of spots/5×10^4 T cells and are subtracted from the background of IFN-γ release by T cells alone. T test was performed to identify statistical differences of the results (* $p < 0.05$)

HLA-I, HLA-II, β2M, TAP-1 TAP-2, LMP2, LMP10, Calnexin and Calreticulin were modulated by HDACi and/or Butyrate (Fig. 4E–H) in CICs. All the co-culture conditions elicited T cell activation against the FBS tumor cells, although with superior levels of IFN-γ release upon the activation of T cells with CICs pre-treated with either Vorinostat or 5-aza (N = 149 and 159 spots /5×10^4 T cells spots, respectively, Fig. 5C, D). Of note, the reactivity against HLA-mismatched (1076 CICs and FBS cell lines) or histologically unrelated tumor cells (Raji) was negligible for all the co-culture conditions although, superior tumor specificity of T cells (absence of non-specific reactivity) was observed for CIC-treated with Vorinostat, 5-aza or Butyrate (Fig. 5C, D).

The co-culture of PBMCs in the presence of CICs treated with miRNA-15a mimics or its combination with IFN-γ plus or minus the IDO inhibitor, 1-MT, was also performed. The overexpression of miRNA-15a led to the induction of T cell mediated immune response towards CICs (Fig. 6A; data are expressed as fold change of cytokine release as compared to UT conditions), only upon pre-treatment of target cells with IFN-γ, with

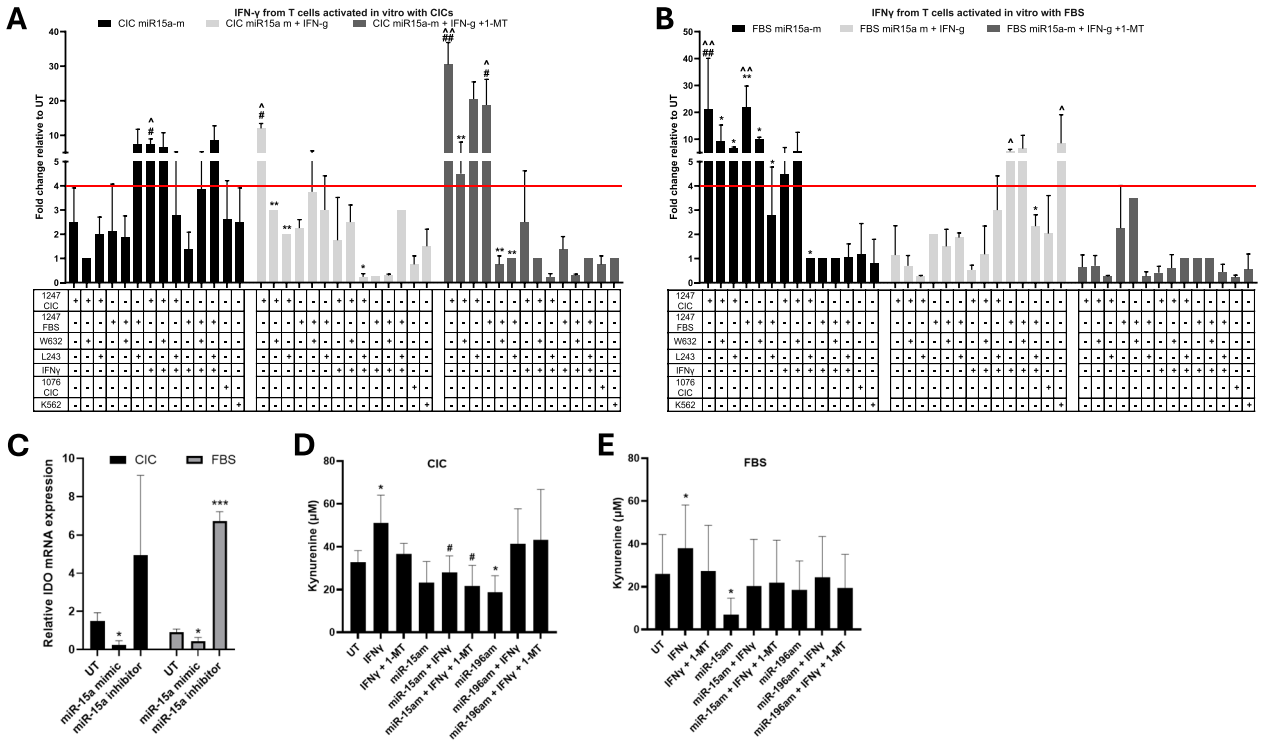

Fig. 6 The role of miR-15a and miR-196a in modulating IDO activity and promoting the susceptibility of CICs to T-cell mediated responses. PBMCs from HLA class I-matched healthy donor (HD) were cultured in vitro with irradiated CRC-CICs (**A**) or FBS tumor cells (**B**) with or without (UT) pre-treatment of the tumor cells with miR-15a mimic alone or in combination with either IFN-γ or IFN-γ plus 1-MT. Following 5 weeks of in vitro culture, the tumor-specific release by T cells of IFN-γ (**A**, **B**) or IL-4 (data not shown) was simultaneously detected by Dual-color EliSpot assay (for details, *see Sect. 2.7 of Materials and Methods*). The HLA class I or class II-restricted T cell responses were determined by using (10 μg/mL) of the blocking mAbs W6/32 and L243 (anti-HLA class I or class II, respectively), in house produced with the specific hybridomas, ATCC, USA). Moreover, target cells (CICs or FBS cell lines) were either untreated or pre-treated with IFN-γ. As controls of antigen-specific reactivity, HLA-mismatched cell line (1076 CIC) or histologically unrelated tumor cells (K562), that are also defective for the expression of HLA molecules, were used as controls. Data was calculated as a mean of two replicates of N. of spots/2.5×10^4 T cells and were subtracted of the spontaneous release (background) of cytokines by the lymphocytes. Data are expressed in the graphs as fold change relative to the corresponding conditions using untreated (UT) tumor cells (either CICs or FBS tumor cells) as stimulators of PBMCs. Thresholds were set based on the number of spots subtracted of background and QC of negative controls of the assays (>N = 4 spots /2×10^4 T). Data were acquired with the ImmunoSpot analyzer Ultimate V6 (CTL). T test was performed to assess the statistical differences between: 1. the reactivity of T cells against CICs or FBS tumor cells along the different MLTCs (^$p < 0.05$; ^^$p < 0.01$); 2. within the same MLTC the reactivity of T cells against target cells (CICs or FBS tumor cells) pre-incubated or not with IFN-γ (# $p < 0.05$); 3. the statistical significant of cytokine release by T cells upon pre-incubation of target cells CICs and FBS (pre-treated or not with IFN-γ) with anti-HLA class I W6/32 or HLA class II L2.4.3 mAbs (*$p < 0.05$; **$p < 0.01$). CRC-CICs and -FBS (N = 3 each) were transfected with mimics or inhibitors of miRNA-15a or 196a (**C**) and the IDO mRNA expression was assessed by qRT-PCR normalized by GAPDH mRNA expression. Graphs are representative of three experiments. **D**–**E** IDO activity in the cell culture supernatants was assessed using a sensitive fluorescence-based bioassay to quantify the concentration of kynurenine in cell culture supernatants collected following 48 h of in vitro culture of the cells. The concentration of kynurenine was determined using a standard curve of twofold dilution of the metabolite and the calculation of the linear regression. Means ± SD values of OD of three replicates were used for the calculation. Statistical significance of differences of the concentration of kynurenine was assessed through T-test by the comparisons of each condition; *$p < 0.05$, **$p < 0.01$, *** $p < 0.001$

inhibition of IFN-γ release in the presence of the HLA-DR blocking mAb (7.4- vs. 2.8-fold change of IFN-γ spots, respectively, $p < 0.05$; Fig. 6A). However, no specific reactivity directed to FBS tumor cells was observed (Fig. 6A, black bars). When CICs pre-treated with both miRNA-15a mimic and IFN-γ were used as source of antigen presenting cells, specific HLA class I and class II-mediated T cell response was induced against these cells, as shown by the inhibition of cytokine release upon the pre-treatment of target cells with specific mAbs (N = 12-, 3- and two-fold change, respectively, $p < 0.05$; Fig. 6A, grey bars). The tumor reactivity was suboptimal (2.25-fold change) towards FBS tumor cells. No augmentation of anti-tumor reactivity was shown upon the incubation of target cells with IFN-γ (Fig. 6A, grey bars). The combination treatment of CICs with miRNA-15a mimic, IFN-γ and 1-MT, elicited the most efficient anti-tumor T cell reactivity which was inhibited by the pre-incubation of target cells

with either anti-HLA-I or anti-HLA-DR mAbs; for CICs: 30.5-, 4.5- and 20.5-fold-change, respectively, $p < 0.05$; for FBS: 18.8-, 0.8- and onefold, respectively, $p < 0.01$) Fig. 6A, dark grey bars). Of note, no further increase of the reactivity was observed when target cells were pre-treated with IFN-γ (Fig. 6A, dark grey bars). Treatment with miRNA-15a mimic also resulted in decreased levels of the gene encoding for the immunomodulating molecule IDO, in both CICs and FBS (fivefold and 2.5-fold, $p < 0.05$, respectively) (Fig. 6C). As a control, the inhibition of the same miRNA led to the induction of the expression of IDO in the same cell lines (3.3-fold, ns and 7.4-fold, $p < 0.001$, respectively) (Fig. 6C). These results were further validated by determining the activity of IDO through the detection of the catabolite product, kynurenine, in the cell culture supernatants upon the transfection or not of both CICs and FBS tumor cells with miRNA-15a or, as control, miRNA-196a mimics. The cell lines were cultured in vitro in the presence of L-tryptophan and were also treated with either IFN-γ or the combination of IFN-γ with 1-MT. Kynurenine was detected in the cell culture supernatants of both types of cell lines, although with superior levels in CICs (32.2 vs. 16.2 μM, in CICs and FBS respectively; Fig. 6D, E), and its concentration was augmented when the cells were pre-incubated with IFN-γ (51.3 and 38 μM in CICs and FBS respectively; Fig. 6D, E). In both cases, the blocking of IDO led to the inhibition, although without statistical significance, of the activity of IFN-γ on the catabolism of tryptophan (31.6 and 27.4 μM, respectively; Fig. 6D, E). MiRNA-15a overexpression reduced the production of kynurenine as compared to baseline levels by the cell lines, although with statistical significance only for FBS tumor cell lines. The levels of kynurenine in the cell culture supernatants of CICs were significantly decreased following the combination of miRNA-15a modulation with either IFN-γ or IFN-γ plus 1-MT as compared to IFN-γ or IFN-γ plus 1-MT alone (Fig. 6D). Similar effects were observed for FBS cell lines, but without statistical significance (Fig. 6E). The up-regulation of miR-196a led to the statistically significant decrease of IDO activity in CICs as compared to baseline, but not when the cells were cultured in the presence of IFN-γ. No statistically significant effect was shown for FBS tumor cells, regardless of the presence or not of IFN-γ (Fig. 6D). These results, taken together, highlight that the modulation of miRNA-15a or its combination with 1-MT, through the simultaneous inhibition of IDO and TGF-β signaling and the up-regulation of the immunogenicity, can induce robust HLA-class I and class II-mediated T cell responses towards CICs.

FBS tumor cells pre-treated with miRNA-15a mimic elicited in vitro T cell-mediated responses (Fig. 6B) against both CICs and FBS target cells, with preferential HLA-DR dependent reactivity (CICs used as target cells: 21-, 9.3- and 6.7-fold-change, respectively, $p < 0.05$; FBS used as target cells: 28-, 10- and 2.8-fold-change, respectively, $p < 0.05$; Fig. 6B, black bars). No further implementation of the reactivity was detected upon combination of treatment with miRNA mimic plus IFN-γ with or without -MT (Fig. 6B, grey and dark grey bars, respectively). This observation can be explained by the lower activity of IDO in FBS as compared to CICs (Fig. 6D, E). Consequently, the modulation of the miRNA-15a is sufficient for the significant inhibition of the catabolism of tryptophan while no effect was observed by other combinations of treatments (Fig. 6E). IL-4 release was also detected in the MLTCs described above, although with suboptimal levels when CICs were used to elicit T cell-mediated responses (*data not shown*).

Phenotype characterization of T cells elicited by the co-culture with CRC cells

CIC-stimulated T cells showed a preferential enrichment of $CD8^+$ T cells (50%) vs. $CD4^+$ T cells (45%) with tumor cells either untreated (UT) or pre-treated with IFN-γ. The frequency of $CD4^+$ T cells was higher for the MLTCs with CICs pre-treated with 5-aza, HDACi or Butyrate (91, 65 and 53%, respectively; Figure S7A). A predominant co-expression of CD95 and CD45RO was observed for both $CD8^+$ and $CD4^+$ T cells from all the types of MLTCs, with higher frequency in UT, IFN-γ, HDACi and 5-aza (Figure S7B-C). Of note, although representing less frequent subsets, $CD8^+CD95^-CD45RO^+$ or $CD4^+CD95^+CD45RA^+$ T lymphocytes were also observed in the MLTCs with UT or 5-aza treated CICs, respectively (Figure S7B-C). The $CD8^+$ or $CD4^+$ $CD95^+CD45RO^+$ T cell subsets were predominantly $CCR7^+CD62L^-$ in all the MLTCs (Figure S7D and G) representing intermediate memory T cells (T_{IM}); however, $CD8^+CCR7^+CD62L^+$ central memory T cells (T_{CM}) were also observed in the T cell populations (4.2, 6.2 or 4.9%, respectively, vs. 1.69% for UT, $p < 0.05$) generated with CICs plus Vorinostat, 5-aza or Butyrate (Figure S7D). This evidence correlates with the superior anti-CIC reactivity in these MLTCs (Fig. 5). $CCR7^+CD62L^-$ were enriched in $CD4^+CD95^+CD45RA^+$ T cell subset in HDACi-, and at lower levels, butyrate-MLTCs (20 and 6.4%, respectively, vs. 2% for the UT, $p < 0.01$ and $p < 0.05$, respectively, Figure S7J). Moreover, $CD279^-CD272^+$ T cells that were found within $CD8^+CD95^+CD45RO^+$ lymphocytes showed an increase of frequency (79.5%, 68.5% and 78.2%, respectively, compared to 62.1% for the UT, $p < 0.05$), in MLTCs with CICs pre-treated with HDACi, 5-aza or Butyrate (Figure S7E). Along this line, the $CD279^+CD272^+$ T cell subset was superior in the MLTCs from IFN-γ treated CICs while a significant decrease in

the frequency of this subpopulation occurred in HDACi and butyrate conditions (35.4% vs.5.4% and 4.1%, respectively, as compared to 13% for UT, $p<0.05$; Figure S7E). Similar results were observed for the frequency of $CD279^{-}CD272^{+}$ T cells within $CD4^{+}$ T lymphocytes, however the lowest frequency of $CD279^{+}CD272^{+}$ T cells was found only for 5-aza- and HDACi-MLTCs (10.8% and 29.6%, respectively, vs. 49.4% for the UT, $p<0.05$, Figure S7H). Within the $CD8^{+}CD95^{+}CD45RA^{+}$ T cells, the subsets of $CD279^{-}CD272^{+}$ were slightly increased in cells treated with 5-aza or Butyrate, as compared to UT or IFN-γ conditions, respectively (1.6 and 2.6% vs. 0.985 and 0.25%, respectively, $p<0.05$; Figure S7I).

Interestingly, MLTCs established with CICs pre-treated with either Vorinostat, 5-aza or Butyrate showed a drop in the frequency of $Tim\text{-}3^{+}CD152^{-}$ and the increase of $TIM\text{-}3^{-}CTLA\text{-}4^{-}$ lymphocyte subsets (for $TIM\text{-}3^{+}CD152^{-}$: 53.2, 59.6, 49.9%, respectively, compared to UT: 71%, ns, ns and $p<0.05$, respectively; for $TIM\text{-}3^{-}CD152^{-}$: 45, 37.2 and 45%, respectively, compared to the UT: 27%, $p<0.05$; Figure S7F).

The enrichment of central memory T cells and of $CD279^{-}CD272^{-}$, $CD279^{-}CD272^{-}TIM\text{-}3^{-}CTLA\text{-}4^{-}$ subsets in MLTCs established with HDACi, 5-aza and Butyrate treatments was associated with increased anti-CIC-specific T cell reactivity (Fig. 5).

Pretreatment of CICs with miR-15a mimic for the stimulation in vitro of PBMCs led to a slight decreased frequency of $CD8^{+}$ T cells compared to UT CICs (41.5 vs. 50.3%, respectively, ns; Figure S8A), which was consistent with the detection of HLA class II-restricted T cell responses (Fig. 6A). Interestingly, the combination of miR-15a mimic with IFN-γ led to a preferential selection (92.1% of positive cells) of $CD8^{+}$ T cells while the combination of miR-15a mimic with IFN-γ and 1-MT resulted in 53.3% of $CD8^{+}$ and 41.7% of $CD4^{+}$ T cells. Surprisingly, all the MLTCs established with FBS tumor cells led to the preferential enrichment of $CD4^{+}$ T cells (Figure S8A). Both $CD8^{+}$ and $CD4^{+}$ T cells were enriched in $CD95^{+}$ $CD45RO^{+}$ subset (Figure S8B-C). Superior percentage of stem memory $CD95^{+}CD45RA^{+}CD8^{+}$ T cells were observed in MLTCs generated with CICs or FBS tumor cells treated with miRNA-15a mimic + IFN-γ, (2.4 and 2.1%, respectively, vs. 0.9 and 0.07% in UT CICs and FBS, $p<0.05$, respectively). $CD95^{+}CD45RA^{+}$ T cells were detected within $CD4^{+}$ subset isolated from the stimulation in vitro with FBS tumor cells treated with miR-15a mimic + IFN-γ (4.5 vs. 0.1% in UT, $p<0.05$; Figure S8C). Interestingly, the $CCR7^{-}CD62L^{-}$ T_{EM} subset was preferentially enriched in MLTCs with CICs treated with either miRNA-15a mimic + IFN-γ or miRNA-15a mimic + IFN-γ + 1-MT (75.2 and 88.5%, respectively, vs. 1.6% in UT condition; $p<0.01$) (Figure S8D and G). $CD8^{+}$ and $CD4^{+}$ lymphocytes co-expressing CD95 and CD45RO and isolated from the MLTCs with CICs pre-treated with miRNA-15a mimic + IFN-γ + 1-MT or with miRNA-15a mimic-FBS, displayed the enrichment of $CD279^{-}CD152^{-}$ and the decrease of the frequency of $CD279^{-}CD152^{+}$ ($CD8^{+}$ T cells: 63.3 vs. 6%, $p<0.01$, and 35.1 vs. 87.2%, respectively; $p<0.05$; $CD4^{+}$ T cells: 88.3 and 91.5% vs. 38.3%, $p<0.05$, and 6.3 and 3.8% vs. 33.4%, respectively, $p<0.01$; Figure S8E and H). Along this line, the increase of the efficiency in eliciting CIC- or FBS-specific T cell responses was observed in these MLTCs (Fig. 6). The detection of $TIM3^{+}CD152^{+}$ T cells in the above MLTCs suggest that this lymphocyte subpopulation might be associated with the activation of tumor specific T cells and not with the late differentiation or anergy of T cells (Figure S8F and I). In summary, the treatment of CICs with miRNA-15a mimic + IFN-γ or with miRNA-15a mimic + IFN-γ + 1-MT resulted in the efficient induction of tumor-specific T cell responses, composed by stem memory and effector memory T cells.

CIC phenotype modulation by miRNAs

The expression of stemness-associated markers was detected in CRC-CICs vs. -FBS and their modulation was detected in tumor cells either UT or transfected with miR-15a or miR-196a mimics or inhibitors. The gating strategy used for flow cytometry analyses to identify subsets of tumor cells according to the expression of markers associated with CRC-CICs (CD24, ALDH-1, LGR5, CD133, CD44v6 and Oct4) is shown in Figure S9. CD24 and ALDH-1 were expressed homogenously in CICs with, as expected, higher levels observed in CICs compared to the autologous FBS tumor cells (Figure S10). CICs were homogeneously composed of $CD24^{+}$ $ALDH\text{-}1^{+}$ cells (99% of positive cells) while lower frequency of these markers in FBS tumor cells (58% of positive cells and threefold and twofold lower RMFI for CD24 and ALDH-1, respectively; $p<0.05$, in FBS tumor cells as compared to CICs) (Figure S10A-B).

Distinct subsets (N = 6) based on the co-expression or not of LGR5, CD44V6 or Oct4 were identified in CRC-CIC lines and the expression of immune checkpoints (CTLA-4, PD-L1 and PD-L2) or immunoregulatory molecules (membrane or intracellular expression of IL-4) were assessed. The expression of CTLA-4, PD-L1 and PD-L2 was found in CICs triple positive for CD44v6, LRG5 and Oct4 (Fig. 7A–D). High frequency of co-expression of PD-L1 with either PD-L2 or CTLA-4 or IL-4 and, with even higher levels of PD-L2 + $IL\text{-}4^{+}$ cells in the same tumor cell subset (Fig. 7A–D). Interestingly, miRNA-15a and miRNA-196a mimics induced a decrease of either $PD\text{-}L1^{+}PD\text{-}L2^{+}$ or $PD\text{-}L1^{+}CTLA\text{-}4^{+}$ cells, and, at a lesser extent, of PD-L2 and IL-4 in CICs

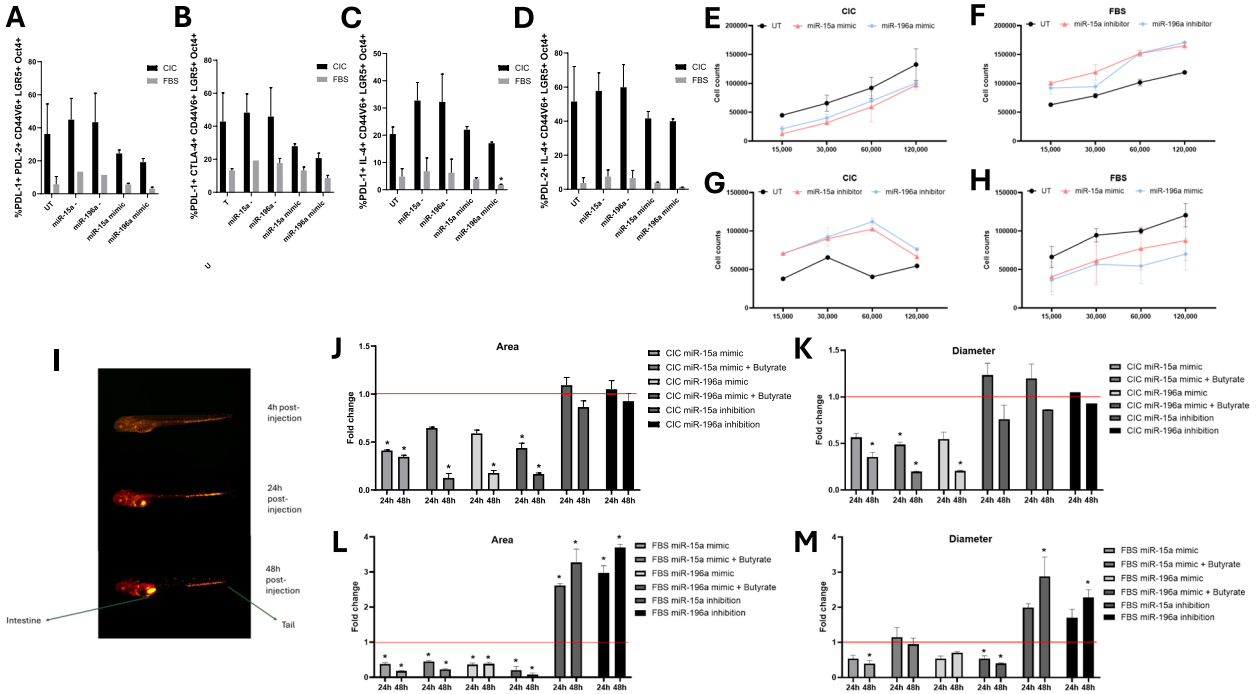

Fig. 7 miR-15a and miR-196a can modulate the expression of immune checkpoints and IL-4 and the proliferation and tumorigenic properties of CICs. The expression of PD-L1, PD-L2, CTLA-4 and IL-4 was assessed by flow cytometry in subsets of CICs and, as control, FBS tumor cells (N = 2 each), according to the co-expression of stemness-associated markers (CD24, ALDH-1, LGR5, CD44V6, Oct4). Tumor cell lines were transfected or not with either miR-15a and miR-196a mimics or inhibitors (50 nM) (**A**–**D**). Data are means of % of positive cells of N = 3 experiments. T test was used to assess the statistical significance of differences of values (*$p < 0.05$, **$p < 0.01$, ***$p < 0.001$). Cell proliferation of tumor cell lines (N = 3) transfected or not with 50 nM of miRNA-15a and -196a mimics or inhibitors was evaluated by DELFIA Cell Proliferation Kit, using 15, 30, 60 or 120 × 10^4 cells/well. Means ± SD values from N = 3 experiments are shown (**E**–**H**). Tumor cell lines (#1247 CICs and FBS) were transfected or not with mimics or inhibitors of miRNA-15a or -196a (50 nM) for 48 h and/or were treated with butyrate (1 mM) (overnight) and then were labeled with 2 ug/mL of DIL and injected (50 cells/nL) in the perivitelline space of 2dpf zebrafish embryos (N = 10–18 embryos for each condition). Cell localization and tumor formation were monitored by fluorescent microscopy (for details, *see Sect. 2.8 of Materials and Methods*). The behavior and migration of tumor cells in the trunk and tail regions of zebrafish have been monitored and representative image of zebrafish embryos showing cell distribution, and formation of tumors after 24 and 48 h of injection are represented (**J**–**M**). Tumor areas (μm^2) (**N**, **O**) and diameters were monitored and analyzed by Zen Blue software (Zeiss) after 4 h, 24 h and 48 h in either the trunk or the tail regions. The area and diameter of tumors within the zebrafish embryos were assessed. Graphs (**J**–**M**) represent the fold change after 24 h and 48 h relative to the 4 h (baseline) and to the UT condition. Means ± SD values from at least two experiments are shown. * Shows the fold change > twofold compared to the untreated condition. *$p < 0.05$, **$p < 0.01$, ***$p < 0.001$

co-expressing CD44v6, LGR5 and Oct4 (24.4 and 19.1%, respectively vs. 36.2% in UT; 27.9 and 20.7%, respectively, vs. 42.8% in UT and 39 and 37.9 vs. 52% in UT; Fig. 7A, B, D). As control, the up-regulation of these immune-related markers was shown by the inhibition of both miRNA-15a and -196a (Fig. 7A–D). The expression of these markers was significantly lower in FBS tumor cells vs. CICs and their modulation by the mimics of miRNAs occurred at suboptimal levels (Fig. 7A–D).

The up-regulation of miRNA-15a and miRNA-196a led to significant decrease of the proliferative ability in vitro, with superior effect by the first miRNA, in both CICs and FBS tumor cells (Fig. 7E, F). On the other hand, miRNA-15a and miRNA-196a inhibition led to a significant increase of the proliferation of these cell lines, with lower extent for FBS tumor cells (Fig. 7G, H). These results suggest that miRNA-15a and -196a exert tumor suppressive functions, with superior activity in tumor cell subsets endowed with superior self-renewal and proliferative properties.

MiRNA-15a and miRNA-196a regulate the in vivo tumor formation and migration

Zebrafish xenograft model was utilized to assess whether the modulation of miRNA-15a or miRNA-196a in association or not with butyrate could affect the tumorigenic capacity and migration in vivo of CICs and FBS tumor cells. Tumor cells were stained with red fluorescent dye (DIL) and inoculated in zebrafish embryos at 2 days post fertilization (dpf). The migration of the cells and

the tumor formation was monitored by fluorescence microscopy at 4, 24 and 48 h. post-injection. Figure 7I shows a representative image of one embryo and the CIC's ability to migrate and metastasize in other organs from the original site of injection. Red fluorescent cells were detected in the intestine, tail and brain of zebrafish (Fig. 7I). The localization, area, perimeter, diameter and intensity of fluorescence of the migrated cells were determined. Embryos injected with CICs showed higher values of area and diameter (similar results were obtained for the perimeter and the intensity of fluorescence, *data not shown*) as measure of cell mass formation compared to FBS tumor cells, suggesting superior tumorigenic properties (Fig. 7J–M; N = 8 larvae/treatment were used). The modulation of miRNA-15a or miRNA-196a with mimic reagents led to a significant decrease of the same parameters at 24 h, and an even higher effect at 48 h post-injection of the cells compared to the UT cell lines (Fig. 7J–M). Moreover, the combination of miRNA modulation plus butyrate resulted in a further reduction of the fluorescence signaling and of the area and diameter of tumor formation (Fig. 7J, K). Similar behavior was observed for FBS tumor cells, although with lower values of area, diameters (Fig. 7L, M) and intensity (*data not shown*). On the contrary, miRNA-15a and miRNA-196a inhibitors did not affect, or even led to an increase of the size of tumor formation. The analyses of specific areas of zebrafish, trunk (including yolk, head and intestine) and tail, allowed to dissect the localization of tumor formation and migration when tumor cells were treated or not with miRNA mimics. Notably, the detection of UT tumor cells at 24 and 48 h post-injection in the trunk region occurred predominantly in the intestine, and, although at lower extent, in the brain of zebrafish. The inhibition of tumor formation was observed at short term upon injection of the cells (4 h), in the trunk part of the fish for CICs treated with miRNA-15a mimic. Even stronger inhibition of the migration of the cells to the tail occurred upon the up-regulation of both miRNA-15a and 196a (as shown by the measurement of the area of tumor cell detection; Fig. 7N). At 24 h post-injection, both tumor formation and migration of the cells were significantly inhibited by both miRNA mimics, but the activity of Buthyrate was observed only for the combination with miRNA-15a (Fig. 7N). Complete abrogation of tumor migration and tumorigenicity was detected at 48 h post-inoculation of the cells by the treatment of miRNA-15a mimic with or without Buthyrate in both trunk and tail regions of zebrafish. Similar behavior of the cells but at a lower extent, was observed for miRNA-196a mimic. The inhibition of tumor formation and migration of the cells to the tail was also detected at 24 and 48 h post-injection of FBS tumor cells with the same treatments, although overall less detection of tumor size (area) was observed (Fig. 7O). Therefore, a specific effect in inhibiting the tumorigenic and migration properties of CICs can be achieved by the up-regulation of the expression of miRNA-15a and miRNA-196a.

Discussion

Cancer is caused by an accumulation of genetic and epigenetic alterations in cells whose undergoing dynamic changes lead to the alterations in pathways regulating the proliferation, growth, programmed cell death, angiogenesis and mobilization. These genetic traits together with the interaction with tumor microenvironment (TME), can determine the heterogeneity of cancer [40]. In this context, CICs represent rare cells endowed with elevated heterogeneity and plasticity that exist in a dynamic equilibrium and continuous crosstalk with the tumor subpopulations and the TME [41]. Additionally, CICs display resistance to standard therapies and immunotherapy through the aberrant activation of molecular pathways and the suboptimal levels of antigen processing and presentation [3–5, 42]. Therefore, dissecting the mechanisms regulating the phenotype and its modulation in this rare tumor subpopulations will contribute to the identification of agents that can efficiently target CICs, the unfavorable TME and their associated immune escape mechanisms [43, 44]. Along this line, CRC patients have been classified based on prognosis and sensitivity to immunotherapy. The gene set enrichment analyses of CRC led to the identification of stemness scores, with the higher stemness scores correlating with worse prognosis, superior infiltration in TME of immunosuppressive cells and lower responses to immunotherapy [45]. However, strategies to revert the immunoresistance of CRC-CICs has not been fully dissected and conclusive results are not yet available.

This study presents the first integrative approach of multi-omics characterization of a large array of primary CICs as compared to the bulk differentiated (FBS) tumor cell lines, and functional in vitro validation of the predicted signatures. Data sets containing large information of genes, miRNAs and methylation (both hypomethylation and hypermethylation) profile at promoter and gene levels were obtained. DEGs analyses identified many molecular pathways that were significantly impacted in CICs, including cytoskeleton and migration, HIF-1, fructose and mannose metabolism, glycolysis/gluconeogenesis, EMT and TGF-β. The association of the data sets from the three platforms allowed the identification of miRNAs and the linked target genes differentially expressed in CICs vs. FBS tumor cells. Moreover, the aberrant expression of these miRNAs correlated with the hypo or hypermethylation of genes and promoters.

Among these, miR-15a-5p and miR-196a-5p were selected as potential modulators leading to a differential behavior of the cells. Aberrant down-modulation of miRNA-15a in tumor tissues vs. adjacent normal mucosa has been associated with progression and worst prognosis of CRC; moreover, the overexpression of this miRNA in CRC cell lines inhibited their proliferation and migration [46, 47]. Furthermore, miR-196a has been shown as overexpressed in different types of malignancies [48–50] and also involved in the regulation of the pathogenesis and the development of cancer [51]. Indeed, the up-regulation of miRNA-15a and miRNA-196a in CRC tumor cells, with superior effect in CICs, led to the regulation of the expression of multiple target genes, that were identified through both prediction bioinformatics tools and the transcriptomics of tumor cells genetically modified for miRNA expression. These genes belong to the TGF-β pathway (*SMAD2/3, JUNB, TGFBR2*), that can regulate either oncogenic features, cell invasion and progression, EMT, evasion from immune responses or the inhibition of tumorigenicity and induction of immune responses (*THBS1)* [52]. On the contrary, the up-regulation of proto-oncogenes was observed upon the inhibition of miRNAs-15a and -196a in CRC-CICs. This evidence, together with the experimental confirmation that these miRNAs were downmodulated in CRC tissues vs. distal normal mucosa, suggests that the observed up-regulation in CICs was only relative to the bulk differentiated cells, and associated with the heterogeneous composition of clonal cells within the tumor tissues. Additionally, for the first time, we showed that the mimic of miRNA-15a can increase, with higher extent in CICs vs. FBS tumor cells, the immunogenicity of CRC cells through the up-regulation of HLA and APM molecules. The efficiency of miRNA-15a in positively regulating the expression of HLA class I, Calnexin and Calreticulin in CICs was superior as compared to the epigenetic regulation of HDACi agents. The transcriptomics of CICs and differentiated tumor cells upon their treatment with these agents or with the combination of IFN-γ plus Buthyrate, mimicking the inhibition of HDACs [53] plus the immunomodulatory activity [54], highlighted the increase of the expression of genes encoding for HLA and APM molecules, as well of NKG2D ligands (*MIC-B* and *ULBP-2*).

These results were corroborated by the activation in vitro of T lymphocytes using CICs pre-treated with epigenetic drugs as source of tumor antigens, showing superior efficiency in eliciting CRC-specific T cell responses as compared to tumor cells treated or not with IFN-γ. Of note, the modulation of CICs and FBS tumor cells with miRNA-15a could elicit anti-tumor T lymphocytes, in line with its effect in up-regulating HLA and APM molecules and down-modulating TGF-β pathways.

IDO is over-expressed by a variety of solid tumors, such as breast, glioma and prostate cancer [55–57] and can also play a role in orchestrating the immunosuppressive properties of CICs [25]. Moreover, IDO1-mediated tryptophan catabolism by tumor cells is inducible by IFN-γ [58, 59]. We showed that the manipulation of CRC-CICs with miRNA-15a mimics can efficiently down-modulate the expression of IDO gene and the combined pre-treatment of these tumor cells with miRNA-15a plus IFN-γ or with the additional inhibitor of IDO1, 1-MT, strikingly increased the efficiency in eliciting in vitro antigen-specific T cell responses. These observations confirmed the relevant role of miRNA-15a in regulating the immunogenicity of CRC-CICs through the simultaneous induction of antigen processing and presentation mechanisms and the neutralization of the immunoregulatory activity of IDO1. Few types of IDO1 inhibitors have been used in clinical studies for the treatment of patients with solid tumors, even in combination with immune checkpoint blockade, however the enthusiasm for these dual therapeutic interventions dropped following the registration of cases of severe toxicities [60]. Nevertheless, the inhibition of IDO warrants further investigation to implement the efficacy of immunotherapy. Along this line, our observations suggest that an appealing approach might be represented by the combined modulation of miRNA-15a. Additionally, this miRNA can also significantly reduce the expression of immune checkpoints (PD-L1, PD-L2 and CTLA-4) and of the immunoregulatory molecules IL-4 in subsets of CICs, as further proof of its ability to counteract the negative immunoregulatory properties of these cells. Our findings further elaborate the sole evidence that miRNA-15a containing vesicles released by mesenchymal stem cells can inhibit the immune evasion of CRC through the regulation of PD-L1 axis [61]. The role of miRNA-15a, either alone or in combination with 1-MT, in augmenting the efficiency CICs in eliciting of anti-tumor T cells was also associated with the enrichment of either central memory or effector memory lymphocyte subsets and the down-modulation of their expression of checkpoints, preventing the differentiation of T cells towards late differentiation or exhaustion. The novelty of our study is the demonstration, through the in vivo zebrafish xenograft model, that the up-regulation of miRNA-15a inhibited the migration and tumorigenic ability of CICs and of differentiated tumor cells. This can be explained, as shown by transcriptomic profiles, by the downstream effect of the down-modulation of genes belonging to either TGF-β pathway or that are involved in proliferation, progression and EMT and the up-regulation of the *THBS1,* a gene involved in the inhibition of tumorigenicity. Interestingly, further inhibition of tumorigenicity and migration in vivo of CICs was

observed upon their pre-treatment with the combination of the mimic of miRNA-15a and Butyrate, along with the action the latest agent, through histone acetylation, in regulating the expression of genes involved in cell differentiation, apoptosis [62], migration and invasion [63]. Moreover, Butyrate can lead to the secretion by CICs of pro-inflammatory molecules (e.g., MIP-1α, MIP-1β and TNF-α, *data not shown*). Thus, Butyrate can enhance the regulation by miRNA-15a of CIC functions.

Ongoing efforts are underway to develop strategies for miRNA therapeutics [64–66]. Although our findings require further translational investigations, restoring miRNA-15a expression in CRC tumor cells, including cell subsets endowed with highest tumorigenicity and resistance to immunotherapy, possibly in combination with immunomodulatory and/or epigenetic agents, can represent an appealing approach to inhibiting tumor formation and invasion and in restoring the susceptibility to T-cell mediated immune responses of tumor cells.

In this study, we show that miRNA-15a enhances the expression of antigen processing machinery and decreases the expression of immune checkpoints (PD-L1, PD-L2, CTLA-4) and immunosuppressive cytokines (IL-4) making the combination of miRNA modulation with existing therapeutic strategies, notably, immune checkpoint inhibitors, a very appealing approach. With recent evidence suggesting that some miRNAs, as complex regulators of gene expression which reflect immune status and activity, can be used to predict the potential clinical benefit of immune checkpoint inhibition therapy [67], these two therapeutic options could be complementary and represent novel investigations for treatments of CRC patients.

Conclusions

Our study demonstrates that modulating miRNA-15a in CICs not only suppresses tumorigenic properties but also enhances their visibility to the immune system by upregulating antigen presentation and reducing immune checkpoint molecules. Notably, combining miRNA-15a modulation with immunomodulatory agents or epigenetic therapies further amplifies these effects, leading to robust tumor-specific immune responses. These findings suggest that targeting miRNA-15a, alone or in combination with other therapeutic strategies, holds significant promise for overcoming treatment resistance in colorectal cancer, potentially improving patient outcomes.

Abbreviations

1-MT	1-Methyl-DL-tryptophan
3′UTR	3′ Untranslated regions
5-aza	5-Azacytidine
AKT3	AKT serine/threonine kinase 3
ALDH-1	Aldehyde dehydrogenase 1
ALDOC	Aldolase C
APM	Antigen presenting machinery
B2M	β2-Microglobulin
BP	Biological process
BrdU	Bromodeoxyuridine
Buty	Butyrate
CHAC1	Glutathione specific gamma-glutamylcyclotransferase 1
CIC	Cancer initiating cell
Col	Colon
CRC	Colorectal cancer
CTLA-4	Cytotoxic T cell antigen-4
CRKL	CRK like proto-oncogene, adaptor protein
DEG	Differentially expressed gene
DGC	Dystroglycan complex
DIL	1,1′-Dioctadecyl-9 3,3,3′,3′-tetramethylindocarbocyanine perchlorate
DNA	Deoxyribonucleic acid
Dpf	Days post fertilization
dUTP	Deoxyuridine triphosphate
EGF	Epidermal growth factor
EGLN3	Egl-9 family hypoxia inducible factor 3
EMT	Epithelial to mesenchymal transition
ENO2	Enolase 2
EPCAM	Epithelial cell adhesion molecule
FBS	Fetal bovine serum
FDA	Food and Drug Administration
FGF	Fibroblast growth factor
FGF19	Fibroblast growth factor 19
FURIN	Paired basic amino acid cleaving enzyme
GAPDH	Glyceraldehyde 3-phosphate dehydrogenase
GE	Gene expression
GSEA	Gene set enrichment analyses
GO	Gene ontology
Gy	Grays
HD	Healthy donor
HDAC	Histone deacetylase
HDACi	Histone deacetylases inhibitors
HIF-1	Hypoxia-inducible factor 1
HKDC1	Hexokinase domain component 1
HLA	Human leucocyte antigen
Hpf	Hours post-fertilization
HSPA5	Heat shock protein family A (Hsp70) member 5
ICAM-1	Intercellular adhesion molecule 1
IDO	Indoleamine 2,3-dioxygenase
IFNGR1	Interferon gamma receptor 1
IFN-γ	Interferon gamma
IL-4	Interleukin 4
IL-7	Interleukin 7
IL-15	Interleukin 15
IL-2	Interleukin 2
INHBB	Inhibin subunit beta B
ITGA1	Integrin subunit alpha 1
JUN B	AP-1 transcription factor subunit
KLRC2	Killer cell lectin like receptor C2
LAG3	Lymphocyte-activation protein 3
LAMA2	Laminin subunit alpha 2
LCK	Src family tyrosine kinase
LGR5	Leucine rich repeat containing G protein-coupled receptor 5
LMP7	PSMB8 proteasome 20S subunit beta 8
logFC	Log2 fold change
LncRNA	Long non-coding ribonucleic acid
MHC	Major histocompatibility complex
MICB	MHC class I polypeptide-related sequence B
MIP-1α/β	Macrophage inflammatory protein-1 alpha/beta
miRNA	Micro-ribonucleic acid
MLTC	Mixed lymphocyte-tumor cell co-cultures
mRNA	Messenger ribonucleic acid
mTOR	Mechanistic target of rapamycin
MUC17	Mucin 17
NANOG	Homeobox protein
NF-κB	Nuclear factor kappa B
NGFR	Nerve growth factor receptor

NKG2D	KLRK1 killer cell lectin like receptor K1
Oct4	Octamer-binding transcription factor 4
OncomiR	Oncogenic miRNA
OS	Overall survival
PBS	Phosphate buffered saline
PCA	Principal component analyses
PCK2	Phosphoenolpyruvate carboxykinase
PDK1	Pyruvate dehydrogenase kinase 1
PDL-1 or -2	Programmed death ligand 1 or 2
PI3K	Phosphoinositide 3-kinase
qRT-PCR	Quantitative reverse transcription polymerase chain reaction
RMFI	Relative mean fluorescence intensity
RNA	Ribonucleic acid
SLC2A1	Glucose transporter protein type 1 (GLUT 1)
SMAD3	Smad family member 3
SOX2-OT	SRY-Box Transcription Factor 2 overlapping transcript
STAT1	Signal transducer and activator of transcription 1
TAP1	Transporter associated with antigen processing 1
TCA	Trichloroacetic acid
TGFBR2	Transforming growth factor beta receptor 2
TGF-β	Transforming growth factor beta
Th	T lymphocyte helper
THBS1	Thrombospondin 1
TME	Tumor microenvironment
TNF	Tumor necrosis factor
TRF	Time-resolved fluorescence
TS-miR	Tumor suppressor miRNA
ULBP2	UL16 binding protein 2
UV	Ultraviolet
Wnt	Wingless-related integration site

Supplementary Information

The online version contains supplementary material available at https://doi.org/10.1186/s12967-025-06176-0.

Additional file 1.

Additional file 2.

Acknowledgements
We thank Advaita Bioinformatics (Ann Arbor, MI, USA) for technical support for bioinformatic analyses.

Author contributions
IT: Data curation, in vitro functional experiments, methodology, writing–original draft; SB: formal analysis of methylation data, investigation, contributing to the writing–original draft. MT: formal bioinformatic analyses of RNA seq and miRNA profiling, data curation, review of the original draft; NG and OH: contributed to phenotype analyses; AS: imaging and data analyses of zebrafish in vivo experiments; ECS: data curation; FR and ARS: data curation of bioinformatic analyses; RM, LM, KW, LL, OS, ST: genomic analyses and data curation, review of the manuscript; WH and SD: methodology for in vivo experiments; YB and NEH: data curation, software; KMH: methodology; SD, KR, PD, GC: data discussion and editing; AT, MT, GS, SF, XW: resources, data discussion and editing. CM: Conceptualization, funding acquisition, supervision, writing–review and editing.

Funding
This study has been funded by the Qatar Research, Development and Innovation (QRDI) grant NPRP10-0129-170277.

Data availability
The data sets and the results generated from this study are available upon request from the corresponding author. Raw and processed sequence read data from the Total RNAseq experiments are available from the corresponding author on reasonable request. Raw and processed DNA methylation, nCounter miRNA profiles, and Lexogen RNASeq data are available at the Gene Expression Omnibus (GEO), series accession number: GSE287214, GSE287585 and GSE287597, respectively.

Declarations

Competing interests
No disclosures were reported by the authors.

Author details
[1]Laboratory of Immune Biological Therapy, Division of Translational Medicine, Research Branch, Sidra Medicine, Doha, Qatar. [2]Jackson Laboratory for Genomic Medicine, Farmington, CT, USA. [3]College of Pharmacy, Qatar University, Doha, Qatar. [4]Advanced Imaging Core, Research Branch, Sidra Medicine, Doha, Qatar. [5]Integrated Genomics Services, Research Branch, Sidra Medicine, Doha, Qatar. [6]Zebrafish Functional Genomics Core, Research Department, Sidra Medicine, Doha, Qatar. [7]College of Health and Life Science, Hamad Bin Khalifa University, Doha, Qatar. [8]Translational Cancer Research Facility, Hamad Medical Corporation, Doha, Qatar. [9]National Center for Cancer Care and Research, Hamad Medical Corporation, Doha, Qatar. [10]Experimental Immunology Unit, Department of Immunology, Transplantation and Infectious Diseases, IRCCS San Raffaele Hospital, Milan, Italy. [11]Department of Health Promotion, Mother and Child Care, Internal Medicine and Medical Specialties, University of Palermo, Palermo, Italy. [12]Department of Precision Medicine in Medical, Surgical and Critical Care, University of Palermo, Palermo, Italy. [13]Department of Surgery, Massachusetts General Hospital, Harvard Medical School, Boston, MA, USA.

Received: 19 December 2024 Accepted: 27 January 2025
Published online: 17 February 2025

References

1. Bray F, Laversanne M, Sung H, Ferlay J, Siegel RL, Soerjomataram I, et al. Global cancer statistics 2022: GLOBOCAN estimates of incidence and mortality worldwide for 36 cancers in 185 countries. CA Cancer J Clin. 2024;74:229–63.
2. Vasan N, Baselga J, Hyman DM. A view on drug resistance in cancer. Nature. 2019;575:299–309.
3. Di Franco S, Mancuso P, Benfante A, Spina M, Iovino F, Dieli F, et al. Colon cancer stem cells: bench-to-bedside-new therapeutical approaches in clinical oncology for disease breakdown. Cancers (Basel). 2011;3:1957–74.
4. Maccalli C, Rasul KI, Elawad M, Ferrone S. The role of cancer stem cells in the modulation of anti-tumor immune responses. Semin Cancer Biol. 2018;53:189–200.
5. Vermeulen L, de Sousa E, Melo F, van der Heijden M, Cameron K, de Jong JH, Borovski T, et al. Wnt activity defines colon cancer stem cells and is regulated by the microenvironment. Nat Cell Biol. 2010;12:468–76.
6. Speigl L, Janssen N, Weide B, Sinnberg T, Pawelec G, Shipp C. Putative cancer stem cell markers are frequently expressed by melanoma cells in vitro and in situ but are also present in benign differentiated cells. Front Biosci (Landmark Ed). 2023;28:193.
7. Takeda N, Jain R, LeBoeuf MR, Wang Q, Lu MM, Epstein JA. Interconversion between intestinal stem cell populations in distinct niches. Science. 2011;334:1420–4.
8. Rotte A, Jin JY, Lemaire V. Mechanistic overview of immune checkpoints to support the rational design of their combinations in cancer immunotherapy. Ann Oncol. 2018;29:71–83.
9. Gajewski TF, Woo S-R, Zha Y, Spaapen R, Zheng Y, Corrales L, et al. Cancer immunotherapy strategies based on overcoming barriers within the tumor microenvironment. Curr Opin Immunol. 2013;25:268–76.
10. Sokol L, Koelzer VH, Rau TT, Karamitopoulou E, Zlobec I, Lugli A. Loss of tapasin correlates with diminished CD8(+) T-cell immunity and prognosis in colorectal cancer. J Transl Med. 2015;13:279.
11. Paulson KG, Voillet V, McAfee MS, Hunter DS, Wagener FD, Perdicchio M, et al. Acquired cancer resistance to combination immunotherapy from transcriptional loss of class I HLA. Nat Commun. 2018;9:3868.
12. Lauss M, Donia M, Harbst K, Andersen R, Mitra S, Rosengren F, et al. Author correction: Mutational and putative neoantigen load predict clinical benefit of adoptive T cell therapy in melanoma. Nat Commun. 2020;11:1714.
13. Ravindran S, Rasool S, Maccalli C. The cross talk between cancer stem cells/cancer initiating cells and tumor microenvironment: the missing

piece of the puzzle for the efficient targeting of these cells with immunotherapy. Cancer Microenviron. 2019;12:133–48.
14. Volonté A, Di Tomaso T, Spinelli M, Todaro M, Sanvito F, Albarello L, et al. Cancer-initiating cells from colorectal cancer patients escape from T cell-mediated immunosurveillance in vitro through membrane-bound IL-4. J Immunol. 2014;192:523–32.
15. Serrano A, Tanzarella S, Lionello I, Mendez R, Traversari C, Ruiz-Cabello F, et al. Rexpression of HLA class I antigens and restoration of antigen-specific CTL response in melanoma cells following 5-aza-2′-deoxycytidine treatment. Int J Cancer. 2001;94:243–51.
16. Luo N, Nixon MJ, Gonzalez-Ericsson PI, Sanchez V, Opalenik SR, Li H, et al. DNA methyltransferase inhibition upregulates MHC-I to potentiate cytotoxic T lymphocyte responses in breast cancer. Nat Commun. 2018;9:248.
17. Pawlak A, Chybicka K, Zioło E, Strządała L, Kałas W. The contrasting delayed effects of transient exposure of colorectal cancer cells to decitabine or azacitidine. Cancers (Basel). 2022;14:1530.
18. Eckschlager T, Plch J, Stiborova M, Hrabeta J. Histone deacetylase inhibitors as anticancer drugs. Int J Mol Sci. 2017;18:1414.
19. Gameiro SR, Malamas AS, Tsang KY, Ferrone S, Hodge JW. Inhibitors of histone deacetylase 1 reverse the immune evasion phenotype to enhance T-cell mediated lysis of prostate and breast carcinoma cells. Oncotarget. 2016;7:7390–402.
20. Slingerland M, Guchelaar H-J, Gelderblom H. Histone deacetylase inhibitors: an overview of the clinical studies in solid tumors. Anticancer Drugs. 2014;25:140–9.
21. Di Tomaso T, Mazzoleni S, Wang E, Sovena G, Clavenna D, Franzin A, et al. Immunobiological characterization of cancer stem cells isolated from glioblastoma patients. Clin Cancer Res. 2010;16:800–13.
22. Lin S, Gregory RI. MicroRNA biogenesis pathways in cancer. Nat Rev Cancer. 2015;15:321–33.
23. Kim J, Yao F, Xiao Z, Sun Y, Ma L. MicroRNAs and metastasis: small RNAs play big roles. Cancer Metastasis Rev. 2018;37:5–15.
24. Sun X, Jiao X, Pestell TG, Fan C, Qin S, Mirabelli E, et al. MicroRNAs and cancer stem cells: the sword and the shield. Oncogene. 2014;33:4967–77.
25. Tomei S, Ibnaof O, Ravindran S, Ferrone S, Maccalli C. Cancer stem cells are possible key players in regulating anti-tumor immune responses: the role of immunomodulating molecules and microRNAs. Cancers (Basel). 2021;13:1674.
26. Maccalli C, Li YF, El-Gamil M, Rosenberg SA, Robbins PF. Identification of a colorectal tumor-associated antigen (COA-1) recognized by CD4(+) T lymphocytes. Cancer Res. 2003;63:6735–43.
27. Todaro M, Gaggianesi M, Catalano V, Benfante A, Iovino F, Biffoni M, et al. CD44v6 is a marker of constitutive and reprogrammed cancer stem cells driving colon cancer metastasis. Cell Stem Cell. 2014;14:342–56.
28. Mennonna D, Maccalli C, Romano MC, Garavaglia C, Capocefalo F, Bordoni R, et al. T cell neoepitope discovery in colorectal cancer by high throughput profiling of somatic mutations in expressed genes. Gut. 2017;66:454–63.
29. Liu X, Xu D, Liu Z, Li Y, Zhang C, Gong Y, et al. THBS1 facilitates colorectal liver metastasis through enhancing epithelial-mesenchymal transition. Clin Transl Oncol. 2020;22:1730–40.
30. Vanhoutte D, Schips TG, Minerath RA, Huo J, Kavuri NSS, Prasad V, et al. Thbs1 regulates skeletal muscle mass in a TGFβ-Smad2/3-ATF4-dependent manner. Cell Rep. 2024;43: 114149.
31. Mehta V, Suman P, Chander H. High levels of unfolded protein response component CHAC1 associates with cancer progression signatures in malignant breast cancer tissues. Clin Transl Oncol. 2022;24:2351–65.
32. Zhang Y, Wang M, Ye L, Shen S, Zhang Y, Qian X, et al. HKDC1 promotes tumor immune evasion in hepatocellular carcinoma by coupling cytoskeleton to STAT1 activation and PD-L1 expression. Nat Commun. 2024;15:1314.
33. Maruyama R, Nagaoka Y, Ishikawa A, Akabane S, Fujiki Y, Taniyama D, et al. Overexpression of aldolase, fructose-bisphosphate C and its association with spheroid formation in colorectal cancer. Pathol Int. 2022;72:176–86.
34. Wang H, Birkenbach M, Hart J. Expression of Jun family members in human colorectal adenocarcinoma. Carcinogenesis. 2000;21:1313–7.
35. Franke FC, Müller J, Abal M, Medina ED, Nitsche U, Weidmann H, et al. The tumor suppressor SASH1 interacts with the signal adaptor CRKL to inhibit epithelial-mesenchymal transition and metastasis in colorectal cancer. Cell Mol Gastroenterol Hepatol. 2019;7:33–53.
36. Janikowska G, Janikowski T, Pyka-Pająk A, Mazurek U, Janikowski M, Gonciarz M, et al. Potential biomarkers for the early diagnosis of colorectal adenocarcinoma - transcriptomic analysis of four clinical stages. Cancer Biomark. 2018;22:89–99.
37. Descarpentrie J, Araúzo-Bravo MJ, He Z, François A, González Á, Garcia-Gallastegi P, et al. Role of furin in colon cancer stem cells malignant phenotype and expression of LGR5 and NANOG in KRAS and BRAF-mutated colon tumors. Cancers (Basel). 2022;14:1195.
38. Yang B, Wu A, Hu Y, Tao C, Wang JM, Lu Y, et al. Mucin 17 inhibits the progression of human gastric cancer by limiting inflammatory responses through a MYH9-p53-RhoA regulatory feedback loop. J Exp Clin Cancer Res. 2019;38:283.
39. Feng Y, Xu Y, Gao Y, Chen Y, Wang X, Chen Z. A novel lncRNA SOX2OT promotes the malignancy of human colorectal cancer by interacting with miR-194-5p/SOX5 axis. Cell Death Dis. 2021;12:499.
40. Dagogo-Jack I, Shaw AT. Tumour heterogeneity and resistance to cancer therapies. Nat Rev Clin Oncol. 2018;15:81–94.
41. Valent P, Bonnet D, De Maria R, Lapidot T, Copland M, Melo JV, et al. Cancer stem cell definitions and terminology: the devil is in the details. Nat Rev Cancer. 2012;12:767–75.
42. Maccalli C, De Maria R. Cancer stem cells: perspectives for therapeutic targeting. Cancer Immunol Immunother. 2015;64:91–7.
43. Yoshida GJ, Saya H. Molecular pathology underlying the robustness of cancer stem cells. Regenerative Therapy. 2021;17:38.
44. Roelands J, Kuppen PJK, Vermeulen L, Maccalli C, Decock J, Wang E, et al. Immunogenomic classification of colorectal cancer and therapeutic implications. Int J Mol Sci. 2017;18:2229.
45. Zheng H, Liu H, Li H, Dou W, Wang J, Zhang J, et al. Characterization of stem cell landscape and identification of stemness-relevant prognostic gene signature to aid immunotherapy in colorectal cancer. Stem Cell Res Ther. 2022;13:244.
46. Xiao G, Tang H, Wei W, Li J, Ji L, Ge J. Aberrant expression of microRNA-15a and microRNA-16 synergistically associates with tumor progression and prognosis in patients with colorectal cancer. Gastroenterol Res Pract. 2014;2014: 364549.
47. Li Z, Zhu Z, Wang Y, Wang Y, Li W, Wang Z, et al. hsa-miR-15a-5p inhibits colon cell carcinoma via targeting CCND1. Mol Med Rep. 2021;24:735.
48. Hui ABY, Shi W, Boutros PC, Miller N, Pintilie M, Fyles T, et al. Robust global micro-RNA profiling with formalin-fixed paraffin-embedded breast cancer tissues. Lab Invest. 2009;89:597–606.
49. Liu X, Lu K, Wang K, Sun M, Zhang E, Yang J, et al. MicroRNA-196a promotes non-small cell lung cancer cell proliferation and invasion through targeting HOXA5. BMC Cancer. 2012;12:348.
50. Sun M, Liu X, Li J, Yang J, Zhang E, Yin D, et al. MiR-196a is upregulated in gastric cancer and promotes cell proliferation by downregulating p27(kip1). Mol Cancer Ther. 2012;11:842–52.
51. Chen C, Zhang Y, Zhang L, Weakley SM, Yao Q. MicroRNA-196: critical roles and clinical applications in development and cancer. J Cell Mol Med. 2011;15:14–23.
52. Yang Y, Ye W-L, Zhang R-N, He X-S, Wang J-R, Liu Y-X, et al. The role of TGF-β signaling pathways in cancer and its potential as a therapeutic target. Evid Based Complement Alternat Med. 2021;2021:6675208.
53. Davie JR. Inhibition of histone deacetylase activity by butyrate. J Nutr. 2003;133(7):2485–93. https://doi.org/10.1093/jn/133.7.2485S.
54. Siddiqui MT, Cresci GAM. The immunomodulatory functions of butyrate. J Inflamm Res. 2021;14:6025–41.
55. Wang S, Wu J, Shen H, Wang J. The prognostic value of IDO expression in solid tumors: a systematic review and meta-analysis. BMC Cancer. 2020;20:471.
56. Prendergast GC. Immune escape as a fundamental trait of cancer: focus on IDO. Oncogene. 2008;27:3889–900.
57. Ozawa Y, Yamamuro S, Sano E, Tatsuoka J, Hanashima Y, Yoshimura S, et al. Indoleamine 2,3-dioxygenase 1 is highly expressed in glioma stem cells. Biochem Biophys Res Commun. 2020;524:723–9.
58. Banzola I, Mengus C, Wyler S, Hudolin T, Manzella G, Chiarugi A, et al. Expression of indoleamine 2,3-dioxygenase induced by IFN-γ and TNF-α as potential biomarker of prostate cancer progression. Front Immunol. 2018;9:1051.
59. Pallotta MT, Orabona C, Volpi C, Vacca C, Belladonna ML, Bianchi R, et al. Indoleamine 2,3-dioxygenase is a signaling protein in long-term tolerance by dendritic cells. Nat Immunol. 2011;12:870–8.

60. Fujiwara Y, Kato S, Nesline MK, Conroy JM, DePietro P, Pabla S, et al. Indoleamine 2,3-dioxygenase (IDO) inhibitors and cancer immunotherapy. Cancer Treat Rev. 2022;110: 102461.
61. Liu L, Yu T, Jin Y, Mai W, Zhou J, Zhao C. MicroRNA-15a carried by mesenchymal stem cell-derived extracellular vesicles inhibits the immune evasion of colorectal cancer cells by regulating the KDM4B/HOXC4/PD-L1 axis. Front Cell Dev Biol. 2021;9: 629893.
62. Supic G, Jagodic M, Magic Z. Epigenetics: a new link between nutrition and cancer. Nutr Cancer. 2013;65:781–92.
63. Wang H-G, Huang X-D, Shen P, Li L-R, Xue H-T, Ji G-Z. Anticancer effects of sodium butyrate on hepatocellular carcinoma cells in vitro. Int J Mol Med. 2013;31:967–74.
64. Fesler A, Liu H, Ju J. Modified miR-15a has therapeutic potential for improving treatment of advanced stage colorectal cancer through inhibition of BCL2, BMI1, YAP1 and DCLK1. Oncotarget. 2018;9:2367–83.
65. Fadaka AO, Akinsoji T, Klein A, Madiehe AM, Meyer M, Keyster M, et al. Stage-specific treatment of colorectal cancer: a microRNA-nanocomposite approach. J Pharm Anal. 2023;13:1235–51.
66. Kim T, Croce CM. MicroRNA: trends in clinical trials of cancer diagnosis and therapy strategies. Exp Mol Med. 2023;55:1314–21.
67. Zhou H, Jia W, Lu L, Han R. MicroRNAs with multiple targets of immune checkpoints, as a potential sensitizer for immune checkpoint inhibitors in breast cancer treatment. Cancers (Basel). 2023;15:824.

Publisher's Note